RESEARCH REPORT

Welding Institute of Canada
Institut de Soudage du Canada

WELDING INSTITUTE OF CANADA
INSTITUT DE SOUDAGE DU CANADA

CONTRACT SERIAL NO. 23440-0-9268-01-SQ

CONTRACTOR: WELDING INSTITUTE OF CANADA

The Effect of Shielding Gas Composition on Mild Steel GMA Weld Composition, Properties, and Porosity

(Theoretical background, experimental results, and proposed future work)

WIC FINAL REPORT RC422/91

Prepared by:

S.A. Gedeon and S.J. Rudd

January 1992

53 pp

MICROMEDIA

HEAD OFFICE / SIÈGE SOCIAL: 391 Burnhamthorpe Road East, Oakville, Ont. L6J 6C9 — (416) 257-9881 Fax: (416) 257-9886
CENTRE DU QUÉBEC / QUEBEC CENTRE: 325 boul. Raymond Dupuis, Mont-St-Hilaire, Qué. J3H 5H6 -- (514) 446-3053 Fax: (514) 446-3055
WESTERN CENTRE / CENTRE DE L'OUEST: c/o Metal Dept. S.A.I.T., 1301-16 Ave. N.W., Calgary, Alta. T2M 0L4 — (403) 284-8522 Fax: (403) 284-7164

Acknowledgements

This project was based on the concerns of the CSA W48.4 committee on "Solid Mild Steel Filler Metals for Gas Shielded Arc Welding". Although WIC prepared and conducted this project, many people had a hand in tailoring it to be of maximum value to Canadian Industry.

In particular, this project could never have been launched without the financial support of CANMET/MTL and the intellectual input of Dr. Mac Braid. CANMET/MTL had a strong input throughout this program in performing compositional analysis without which this program could not have been as meaningful.

Additionally, L-TEC, Hobart, Canadian Liquid Air, and Stelco offered materials and valuable input into the program. Dr. Vivek Vaidya deserves thanks, not only as the W48.4 committee chairman, but also for validating the WIC findings in the CLA labs.

Finally, WIC would like to thank its Research Board and the entire membership for supporting this WIC CORE Research Project.

WIC is proud to be able to initiate this major new program which will eventually lead to a predictive capability for selecting shielding gas, filler metal--base metal combinations. The proposed future work in this report will form the basis for continuing industrial involvement.

93-01554/

TABLE OF CONTENTS

Abstract 1

Objective 2

Introduction 2

Background and Theoretical Considerations 3

A) Electrode Tip Reactions 5

B) Reactions Occurring within the Arc Plasma 5

C) Reactions Occurring in the Hot Part of the Weld Pool 5

D) Reactions Occurring in the Cool Portion of the Weld Pool 6

Previous Experimental Results 8

Experimental Procedure 10

Experimental Results 11

Discussion 12

Conclusions 15

Proposed Modifications to CSA W48.4 16

Proposed Future Work 17

References 19

TABLES

Table 1	GMAW Electrode Compositions used in this Study
Table 2	Steel Compositions used in this Study, Base Plate: CSA G40.21 Gr. 44W
Table 3	Test Matrix and Mechanical Test Results
Table 4	Weld Metal Composition vs. Gas Composition

FIGURES

Figure 1	Weld Quality vs. Percent Oxygen
Figure 2	Weld Quality vs. Percent Carbon Dioxide
Figure 3	UTS and Yield Strength vs. Percent CO_2
Figure 4	UTS and Yield Strength vs. Percent CO_2 (S-6 Wire Only)
Figure 5	Charpy Impact Energies vs. Percent CO_2
Figure 6	Charpy Impact Energies vs. Percent CO_2 (S-6 Wire Only)
Figure 7	UTS and Yield Strength vs. Group Index ($GI = \%O_2 + 1/2\%CO_2$)
Figure 8	Charpy Impact Energies vs. Group Index ($GI = \%O_2 + 1/2\%CO_2$)
Figure 9	Charpy Impact Energies vs. Group Index ($GI = \%O_2 + 1/2\%CO_2$)
Figure 10	Weld Metal Carbon vs. Shield Gas CO_2
Figure 11	Weld Metal Silicon vs. Shield Gas CO_2
Figure 12	Weld Metal Oxygen vs. Shield Gas CO_2
Figure 13	Weld Metal Carbon vs. Shield Gas Oxygen
Figure 14	Weld Metal Silicon vs. Shield Gas Oxygen
Figure 15	Weld Metal Oxygen vs. Shield Gas Oxygen
Figure 16	Weld Metal Oxygen vs. Group Index
Figure 17	Weld Metal Carbon vs. Group Index
Figure 18	Weld Metal Silicon vs. Group Index
Figure 19	Micrograph of Specimen #1 (100% CO_2, S-6) 150X
Figure 20	Micrograph of Specimen #22 (50% CO_2, Bal.Ar, S-6) 150X
Figure 21	Micrograph of Specimen #6 (15% CO_2, Bal.Ar, S-6) 150X
Figure 22	Micrograph of Specimen #3 (5% CO_2, Bal.Ar, S-6) 150X
Figure 23	Micrograph of Specimen #7 (2% O_2, Bal.Ar, S-6) 150X
Figure 24	Micrograph of Spec. #13 (2% O_2, 10% CO_2, 30% He, Bal.Ar, S-6)150X
Figure 25	Macrograph of Specimen #1 (100% CO_2, S-6)
Figure 26	Macrograph of Specimen #22 (50% CO_2, Bal.Ar, S-6)
Figure 27	Macrograph of Specimen #6 (15% CO_2, Bal.Ar, S-6)
Figure 28	Macrograph of Specimen #3 (5% CO_2, Bal.Ar, S-6)
Figure 29	Macrograph of Specimen #7 (2% O_2, Bal.Ar, S-6)
Figure 30	Macrograph of Specimen #13 (2% O_2, 10% CO_2, 30% He, Bal.Ar, S-6)
Figure 31	Effect of Shielding Gas Composition on Difference in Haz

The Effect of Shielding Gas Composition on Mild Steel GMA Weld Composition, Properties, and Porosity

(Theoretical background, experimental results, and proposed future work)

WIC FINAL REPORT RC422/91

S.A. Gedeon and S.J. Rudd

January 1992

Abstract

Mild steel gas metal arc welding electrodes are certified in North America with multipass weldments performed using 100% CO_2 and tested in accordance with CSA W48.4 or AWS A5.18. Once the performance criteria are met, the electrodes are also granted certification for use with certain other shielding gas compositions as specified in the standards.

These acceptable composition ranges have recently been called into question and this experimental program was initiated to determine the range of acceptable shielding gas compositions which still meet the required weld performance criteria. Over 40 CSA W48.4 weld qualification plates were welded and tested with O_2 from 0-10%, CO_2 from 0-100%, He from 0-30%, and balance argon. Binary, ternary, and quaternary mixtures were tested with ER 480S-3 (70S-3) and ER 480S-6 (70S-6) GMAW electrodes.

The most significant and previously unreported discovery is that low oxidizing potential shielding gases (from 1-5% O_2 or CO_2) produce unacceptable porosity in multipass weldments with the wire and base metal compositions used in this study. These results have since been verified at other laboratories. The tensile strength, impact toughness, porosity, and weld metal composition and microstructures are also reported in this study as a function of shielding gas composition.

Thermodynamic gas-metal reaction theories and previous IIW experimental results are extensively reviewed to develop an understanding of these results. In addition, proposed future work is discussed which should be undertaken to develop a predictive ability to select acceptable shielding gas - filler metal - base metal combinations.

These results are of interest to the structural and pipeline fabrication community due to the fact that there is a great deal of interest in using lower oxidizing potential shielding gases in multipass applications in order to increase impact toughness.

Objective

The objective of this program is to experimentally examine the effect of systematic variations in shielding gas composition on weld metal composition and properties using C-Mn-Si wires of two CSA W48.4 classifications (ER480S-3 and ER480S-6). Previous experimental results and thermodynamic gas-metal reaction theories are to be reviewed in order to develop recommended changes to the range of shielding gas compositions accepted in CSA W48.4.

Introduction

An inert shielding gas is used during GMAW to protect the molten weld pool and electrode droplets from oxygen and nitrogen contamination from the atmosphere. Oxygen and/or CO_2 are added to the argon or helium shielding gas during GMAW of steel to promote favourable arc characteristics and weld bead shape. In order to prevent porosity and increase weld properties, deoxidizers and other elements are added to the filler metal electrodes. The resulting oxides act as nucleation sites for the transformation of microstructural constituents such as acicular ferrite from austenite and significantly affect weld properties.

Thus the various mechanisms of element transfer and reactions become very important in order to rationally match the base metal, filler metal, and shielding gas chemistry and produce the optimum microstructure and properties.

The fundamental mechanisms of gas-metal reactions occurring during welding have been studied by a number of researchers, however, their results were often contradictory and did not contribute substantially to a rationale for selecting optimum shielding gas-filler metal-base metal combinations. In the early to mid 70's, the International Institute of Welding (IIW) attempted to develop a standard for choosing shielding gas - filler metal combinations. This effort was hampered by the fact that most of the experimental work was carried out in a large number of laboratories in different countries using different parameters and materials on a voluntary basis. The International Standards Organization (ISO) has adopted a shielding gas classification system based on this work, but shielding gas - filler metal combinations have not been standardized.

In North America, no serious effort has been made to match the shielding gas composition to the filler or base metal. In fact, the CSA and AWS standards concerning this have recently been called into question. This project is a direct result of the concerns of the CSA W48.4 committee to determine exactly what shielding gas compositions should be allowable in their standard W48.4 governing GMAW filler metal electrodes for welding mild steel.

Even more important is the need to determine a more general description of how gas-metal reaction analysis as it relates to welding can be used to develop a predictive capability for selecting other filler-base metal combinations and also apply this analysis to other welding processes such as FCAW.

Background and Theoretical Considerations

Most investigations on the effect of shielding gas composition have studied the influence on arc voltage, current, deposition rate, and bead-on-plate weld profiles.

Gilde (1) was probably the first investigator to consider in any detail the gas-metal reaction thermodynamics associated with GMAW. He did not realize or account for the very high temperatures associated with arc welding, however, nor examine the fact that gas-metal reactions will take place at both the electrode tip and in the weld pool.

Pollard and Milner (2) examined the "effective reaction temperature" associated with element transfer during GMAW in 1971. They performed measurements of element transfer during static pool melting using GTAW in an enclosed chamber, as well as moving GTA and GMA welds. Additionally they performed these experiments with relatively pure iron, iron-1% silicon, mild steel, and stainless steel. All experiments were performed using only 100% CO_2, thus the effect of variations in $\%CO_2$, $\%O_2$, or helium were not investigated.

They found that oxygen absorption as a function of time was linear, however, they measured oxygen pickup through weight gain or visual examination of the number of oxide inclusions and slag rather than using the vacuum fusion method currently used (for example by the Leco oxygen-nitrogen analysis unit). They also found that oxygen absorption occurred 50 times faster than carbon absorption. Although they did not attempt to explain this incredible difference in absorption rates, they related the total amount of carbon transfer to the equilibrium amount as predicted by assuming either 100% CO_2 or 100% CO in contact with the weld pool and concluded that the effective equilibrium reaction temperature was about 2200°C in contact with 100% CO_2. They did not consider what the reaction temperature of oxygen absorption would have been (nor why it would have been so different). Additionally they did not consider the possibility of there being both CO and CO_2 present above the weld pool.

Their results on moving GTA and GMA welds concluded that the effective reaction temperature decreases with travel speed. They also claim that the rate of oxygen and carbon transport within the molten weld pool is different. Although this can be one explanation of their experimental results, they do not mention how these differences in reaction temperature or transport rates could be theoretically justified. They also found that GMAW produces a greater propensity for porosity due to the added turbulence increasing nucleation of bubbles and transport of carbon and oxygen to the developing pores.

Examining the effect of silicon, they assumed that all of the reactions occurred during droplet transfer and neglected weld pool reactions from contributing to the final values of element transfer. Assuming pure CO_2 they calculated that the effective reaction temperature at the droplet was 2500°C to 2700°C (although in the conclusions they change this value to 2400°C to 2500°C. They also changed the weld pool reaction temperature from 2200°C to 2300°C without explaining the change).

Coe and Moreton (3) developed a thermodynamic model based on empirical results employing both argon rich and CO_2 rich gas mixtures in 1979. A considerable portion of their work was spent on an analytical oxygen analysis which was far superior to the earlier works in that they used a Leco TC30 with vacuum fusion extraction at 2700°C. However, their model considered the effect of silicon (and less importantly manganese) to be of minor importance and did not examine their losses.

This failure to consider the effect of silicon was based on their assumption that Si will play no role in oxygen absorption or loses, but will only govern the form of the oxides in the solidified weld. However, earlier work by Heile and Hill (4) showed that SiO and SiO_2 losses from the droplet contribute significantly to fume generation and thus also to the amount of oxygen in the droplet.

Coe and Moreton considered only the Fe-C-O system and then compensated for the discrepancy with the empirical results by determining an 85% dissociation of CO_2 into CO. Even though their calculated 85% dissociation (at 1600°C!) is in disagreement with known thermodynamic data, they claim that the arc somehow increased this value. Their calculated effective reaction temperature varies from 1600°C to about 1800°C depending on whose results and which analysis they use. Their primary objective was to use their model to determine appropriate shielding gas-filler metal combinations, which they were unable to do.

Svecinskij and Rimskij (5) primarily evaluated the effect of gas composition on droplet transfer, but also analyzed the gas-metal reactions occurring in 1982. They found that the oxygen in the metal droplet was greater than in the weld pool and that current and voltage had no effect on these values. They postulate that "the action of the magnetic field of the welding current renders possible a separation (segregation) of the components of the gas mixtures which leads to a raising of the concentration of the oxygen close to the molten droplets and can thereby increase its absorption and consequently lower the surface tension of the molten metal." A more likely explanation is not some mysterious segregation, but dissociation of oxygen due to the high arc plasma temperatures.

Perhaps the best experimental work yet performed on gas-metal reactions occurring during GMAW was done by Grong and Christensen (6) in 1983. They used a rotating water-cooled copper wheel cathode to rapidly quench the transferred droplets, and compared these results to electrode tip values and multipass weldments. They used these results to develop a model which examined the gas-metal reactions occurring at the electrode tip, in the arc plasma, and in the weld pool. Welding was performed with both Ar-O_2 and Ar-CO_2 gas mixtures.

Grong and Christensen's analysis and model is the most comprehensive performed to date and can be broken down for a more complete review as follows:

A) Electrode Tip Reactions

They calculate an average electrode tip temperature of 1600°C and postulate that oxygen is absorbed from the shielding gas to form CO and manganese silicate slag. Thus they state that the major carbon loss occurs at this stage, and as a result of the CO evolution, some silicon is lost as SiO to form fume.

Unfortunately, since they did not measure the oxygen, silicon, or manganese losses in the electrode tip, this analysis cannot be validated. The loss of SiO as fume agrees with the work of Heile and Hill (4); however, Heile and Hill's data indicate that silicon losses continue to increase as the $\%CO_2$ in the shielding gas increases which is in contradiction to Grong and Christensen's results which show that carbon losses do not increase beyond 10% O_2 or 20% CO_2 (whereas the silicon losses from Heile and Hill double from 25% CO_2 to 100% CO_2). Also, Grong and Christensen's own experimental results don't agree with this analysis since they found that silicon loses in Ar-O_2 mixtures were greater than in Ar-CO_2 mixtures (even though they state later that these loses should be greater in Ar-CO_2 mixtures based on this mechanism of silicon loss).

B) Reactions Occurring within the Arc Plasma

They calculate an average droplet temperature of about 2400°C and state that oxygen pickup does not occur because Fe and Mg vapours will protect the molten droplet. They claim that the vapour will react with the shielding gas oxygen to form fumes (but that this reaction does not involve the droplet itself but takes place removed from it in the arc plasma). There are a number of locations where they contribute the rate controlling reaction to gas diffusion across a stagnant boundary layer. However, given the fast droplet speeds and arc plasma jets, it would indeed be surprising if there was a significant gas boundary layer which would inhibit reactions. A more likely explanation might be that oxygen from the shielding gas does in fact react with the Fe and Mn in the droplet.

Actually, these experimental results are in direct conflict with those of Svecinskij and Rimskij (5) who found that there was greater oxygen in the droplet as mentioned previously.

C) Reactions Occurring in the Hot Part of the Weld Pool

Grong and Christensen calculated the reaction temperature for this region to be 1800°C to 2000°C. However, recent theoretical calculations based on evaporative mechanisms by Block-Bolten and Eagar (7,8) and more recent experimental results produced by Krause in 1987 using laser interferometry show that this value should in fact be closer to 2300°C.

Additionally Grong and Christensen's calculated temperatures assume that oxygen is controlled by absorption of O_2 or CO_2 and neglects to consider the effect of high temperature dissociation which occurs in the arc plasma.

Instead they postulate a stagnant boundary layer rate controlling step based on the fact that the oxygen absorption varies linearly with the $\%O_2$ in the shielding gas (they make the same assumption in the droplet stage as well). However, if monatomic oxygen was in contact with the weld pool, then this would be another justification for the linear dependence of oxygen absorption.

Grong and Christensen also postulate that manganese silicate slag precipitation takes place at this stage which prevents the oxygen concentration from exceeding a certain limit. However, they fail to describe why the carbon level of the chilled metal and weld pool increases during this stage.

D) Reactions Occurring in the Cool Portion of the Weld Pool

This temperature region is defined by Grong and Christensen as being below 1800°C (the solidification temperature is slightly above 1500°C). Silicon and manganese react further with dissolved oxygen in this stage. However, they state that since slag separation is unfavourable due to the stagnant condition of the bath, that the analytical oxygen content determined will be high and rather unpredictable. These assertions are not consistent with recent fluid flow modelling efforts which show the weld pool to be quite turbulent. Additionally, since the oxygen analysis performed by the vacuum extraction technique measure both the dissolved oxygen and oxide content, the ability to separate slags will have no effect on the amount analyzed.

Thus, although the experimental work of Grong and Christensen is extremely valuable, the theoretical analysis, while being the most complete to date, leaves many questions unanswered. The analysis makes no predictions concerning acceptable base metal-wire-gas combinations. Additionally, the experimental results need to be expanded to determine the effect of various filler metals and the effect of droplet size and welding parameters as well as the effect of helium.

Meyendorf (9) examined the effect of high temperature dissociation of CO_2 and O_2 on oxygen absorption in 1987. He assumed that dissociation and absorption take place at the same temperature. Also, even though he states that his ternary dissociation diagrams fail to consider the fact that there will be about 10% monatomic oxygen present, he neglects to take this into account during the ensuing analysis. Additionally, even though he realizes that oxygen absorption will take place at various locations and temperatures, he performs all his calculations at 2700°C (which he had previously calculated as the temperature of the metal droplet).

The greatest contribution of this work to the field of weld gas-metal reactions is his ternary dissociation diagrams and his figures showing that oxygen content is a linear function of the amount of oxygen partial pressure. Unfortunately he neglects to consider monatomic oxygen absorption and some of his figures showing oxygen partial pressure as a function of $\%CO_2$ in the shielding gas appear to be in conflict with his earlier ternary dissociation diagrams. In contradiction with Grong and Christensen, Meyendorf claims that Mn and Si losses are caused by evaporation of volatile oxides.

One significant shortcoming of virtually all the thermodynamic analyses performed to date is the implicit assumption of local thermodynamic equilibrium (LTE). However, due to the extremely large temperature gradient from the weld pool surface to the arc plasma, reactions occurring in or near the cathode boundary layer will not be at LTE.

The vast majority of arc plasma physics research has been performed on the anode boundary layer rather than the cathode due to the added complexity of the cathode region. Quigley (10) however, has estimated the cathode boundary layer to be about 10^{-3} mm thick and calculates that the temperature immediately above this layer must be at least 8000K in order to ionize the gas so that current can flow across the arc.

Gedeon (11) has reviewed the arc physics literature as it relates to deviations from LTE in the anode and cathode fall regions and found that the ion recombination free path will in general exceed the energy exchange free path (roughly equivalent to a thermal boundary layer thickness) (12). Thus high temperature ions in the arc plasma can arrive at the weld pool prior to losing all of their thermal energy. In practise this means that the deviation from LTE can be analyzed by assuming that the dissociation temperature is effectively higher than the absorption temperature. Drawing this analysis further, Gedeon showed that hydrogen dissociation is governed by the temperature of the cathode boundary layer and that both monatomic and diatomic hydrogen absorption is governed by the temperature of the molten weld pool (11,13). This new two-stage thermochemical analysis was used to explain why previous analyses predicted impossibly high hydrogen absorption temperatures.

A similar analysis as it relates to monatomic oxygen absorption should be performed. Additionally, the effect of low oxygen partial pressures on dissociation should be calculated (all of the previous results have been calculated assuming atmospheric pressure, except Meyendorf).

If one assumed that the CO_2 and O_2 dissociation was controlled by the arc plasma (or cathode boundary layer) temperature rather than the molten weld pool temperature, then the monatomic oxygen present could account for not only the fact that there is a linear dependence of oxygen content on $\%O_2$ in the shielding gas, but that this could also potentially account for the fact that all of the previous researchers have calculated such radically different reaction temperatures (because their calculations were based on the incorrect assumption of either CO_2 or O_2 absorption rather than a combination of CO_2, CO, O_2, and O absorption). Since we now have a better knowledge of the surface temperature of the weld pool, we can use the actual temperature rather than trying to calculate it based on assumptions concerning which reactions are occurring.

These concerns, coupled with recent advances in other areas of welding , can be used to develop a more detailed understanding of GMAW gas-metal reactions. This analysis could then be used to predict acceptable shielding gas - filler metal - base metal combinations.

Previous empirical approaches to the selection of acceptable combinations will now be reviewed.

Previous Experimental Results on Acceptable Shielding Gas - Filler Metal Combinations

In 1970 the IIW submitted a classification system, IIW Doc. XII-B-75-70, for filler wires used in GMAW (referred to as gas shielded metal arc) to ISO (14). It was recognized, however, that since the mechanical properties were known to be directly related to the chemical composition of the weld metal, factors affecting the transfer of elements from the wire to the weld pool were also important. These factors were shown to be mainly shielding gas composition and the welding conditions affecting droplet transfer rate.

Throughout the 1970's, IIW Sub-Commission XII-B conducted a collaborative program in order to draft an ISO standard to link GMAW (or MAG) shielding gases and filler metal electrodes. During this time many publications concerning various aspects of the program were produced (14-19). In 1977 a recommended classification (20, 21) was drafted in IIW Doc. XII-669-77 which classified the shielding gases on the basis of their oxidation potential. Unfortunately this classification was not tied into the filler metal classification scheme and recommended combinations were not made.

The shielding gas classification system was based on a series of about 46 welds made in 8 countries. Although the final recommendations in IIW-669-77 show some experimental results which indicate clear trends, an analysis of the original IIW documents (14-19) shows that the actual scatter in data was much more significant. Much of the numerous directly contradictory data can be attributed to the fact that different parameters, testing procedures, and gas compositions were used from country to country and that no single lab produced more than a handful of data.

For example, Pomaska (18) found that the oxidation potential of O_2 was 10 times that of CO_2 whereas Shackleton (17) found that it was only 2 times as great (for up to 15%CO_2). Coe and Moreton (3) found that CO_2 was more oxidizing than O_2 and also concluded that the presence of O_2 in Ar-CO_2-O_2 mixtures had little effect! Others outside of the IIW, for example Francis, et al (22) who also included the effect of oxygen in the base plate (not done in the IIW study), found that oxygen transfer may in fact be positive or negative depending on the shielding gas oxygen concentration.

Ruckdeschel (15), the Rapporteur of the project, provided the most detailed analysis of the IIW program and produced some very interesting statistical results. For example, the oxygen analysis from nominally identical tests had an average difference of 37% and the average

difference in silicon losses were 114% (note that this is the average difference and that some differences were much more extreme!). He deduced that it was not possible from the data to correlate the oxidizing potential of CO_2 and O_2. In fact, by comparing the amount of dissociation of various mixtures he states, "It can be assumed that the oxidation potential is not a function of O_2 concentration but of O concentration. This would mean that the specific oxidation potential will increase in binary Ar-O_2 mixtures with a reduction of O_2 fraction." It is interesting to note the importance Ruckdeschel places on monatomic oxygen absorption while Grong and Christensen and others have failed to consider this important mechanism of oxygen absorption.

The Ruckdeschel analysis is too confusing and detailed to fully review here, but a number of salient comments of his should be noted. He determined that shielding gases should fall into 8 separate classes (whereas the final IIW document proposes only 5). He shows that gases should not be classified only in terms of oxidizing potential, but also in terms of positional capability, danger of porosity, weld shape and penetration, and fume formation. Finally he shows that voltage differences from lab to lab could account for more differences in oxidizing potential than previously expected, and that oxidizing potential increases much more at low values of O_2 and CO_2 than at higher values.

In spite of all the contradictions and scatter in results, the IIW document recommended the classification of gas compositions based on the simple formula:

$$\text{Group Index} = \%O_2 + 1/2\ \%\ CO_2$$

Although this classification does not coincide as well with the typical weld metal oxygen concentrations as a previous version of the classification, 5 groups were established as follows (also shown are rough approximations of the weld metal oxygen contents based on using a wire with 0.02% oxygen):

I	group index	< 1	Approx. weld oxygen 0.02%
M1	group index	1-5	Approx. weld oxygen <0.03%
M2	group index	>5-9	Approx. oxygen 0.03- 0.05%
M3	group index	>9-16	Approx. weld oxygen >0.05%
C	group index	>16	" "

The most recent discussion concerning this classification system has been put forth by Shackleton and Smith (23) in 1984. They reviewed a number of papers published since the 1977 document and concede that the classification system is limited, but that it is justified as providing general rather than definitive guidance. Some slight revisions to the previous document are recommended.

It should be noted in closing, that the effect of helium has never been established within the IIW.

Experimental Procedure

Based on an analysis of previous work, it was apparent that it was imperative for all of the experimental work to take place within a single laboratory. Additionally the welding parameters and experimental procedure needed to be closely controlled.

All of the ER480S-3 and ER480S-6 filler electrodes used were from the same supplier and each electrode type was from a single heat. The electrode compositions and heat numbers are shown in Table 1. An additional composition analysis was performed on the electrodes used and these values are also shown in Table 1.

Mechanized GMA welding was performed using a Linde VI-450SS constant voltage power supply and an L-Tec Digamatic I controller with a mechanical carriage and side beam. Welding set-up parameters were monitored with CRC Evans data acquisition monitoring equipment to ensure that the parameter settings were accurate. This mechanized setup and data acquisition ensured that operator variability was minimized.

All of the base plates were from a single heat of CSA G40.21-300W steel (roughly equivalent to A36), the composition of which is shown in Table 2. All plates were flame cut and then milled to provide a clean bevel and weld toe surface.

All geometries and welding parameters were based on CSA W48.4 except that the plates were 500mm long rather than 250mm. Thus there was enough weld metal to machine three tensile specimens (rather than only one) and five charpies as well as metallographic and composition samples.

The WIC computerized gas mixing system was used to accurately control the shielding gas composition. The Environics 2000 system consists of a series of 8 linear mass flowmeters with backpressure sensing, a mixing chamber, accumulator, and computer control. The extreme accuracy of the system is based on the principle of each linear mass flowmeter monitoring the amount of thermal transfer of the gas which is dependent on the gas thermal conductivity and varies linearly with flowrate over the upper 90% of the flow range. Thus, by knowing the thermal conductivity of a given gas, the pressure differential and the temperature, the flow rate can be determined with extreme accuracy and repeatability.

Diffusible hydrogen analysis was performed in accordance with AWS A4.3-86 using an Oerlikon Yanaco Model G1106H diffusible hydrogen analyzer based on gas chromatography.

Tensile testing, charpy testing, radiography and chemical analyses were performed in accordance with CSA W48.4. Additionally, oxygen and nitrogen analysis was performed on each weld specimen using a Leco TC 30. Oxygen and nitrogen analysis specimens were either machined into solid 1-gram cylinders from fractured tensile specimens, or obtained by drilling into the weld deposit (it was later determined that the drillings were unacceptable).

Experimental Results

The test matrix of shielding gas compositions and electrodes used as well as mechanical test and radiographic results are shown in Table 3. In order to prevent the chronological order of testing from influencing the results, the order of testings was selected at random (thus the weld specimen numbers were given chronologically and appear randomly in the table).

The most significant and previously unpublished discovery is that low oxidizing potential shielding gases cause porosity in multipass welds with these filler metal - base metal combinations. This is especially disconcerting since CSA W48.4 expressly allows the use of 1-5% O_2-Ar for welds qualified with 100% CO_2.

After the first few low oxidizing potential gas welds failed radiographic examination, a large number of experimental variations were attempted to eliminate the problem. Increased shielding gas flow rates of 40, 50, and 60 cfh were attempted with no success. Bottled gas mixtures were used and different electrode wires were tried in order to eliminate the problem. Variations in welding parameters were also tried to no avail. Another literature survey was performed only to find that nothing like this had been previously published. The only reference was that a few of the IIW test results had been discarded due to porosity and that these had been at 2% O_2-Ar, however, they merely discarded the tests rather than examine why the porosity had occurred.

Further investigation found that the Canadian Welding Bureau (CWB) had never qualified any company to perform multipass GMA welding with low oxidizing shielding gases (in spite of the CSA allowal of these gases). Most companies apparently use these gases for fillet welds and single pass applications.

The Canadian Liquid Air (CLA) laboratory in Montreal then reproduced and validated the WIC results using both 1.2mm and 1.6mm electrodes. Additionally, Linde confirmed their experience with porosity using low oxidizing potential gases in multipass applications.

Figure 1 graphically represents the weld quality (whether the weld passed or failed the radiographic requirements in CSA W48.4) as a function of up to 10% O_2 in the argon shielding gas. Also shown in the upper and middle set of boxes is the effect of adding 5% or 30% helium to the argon (both of these welds failed as well).

Figure 2 shows the weld quality as a function of up to 100% CO_2 in the shield gas (binary CO_2-Ar mixtures shown in the lowest set of boxes). As can be seen by examining the second and third from the bottom set of boxes, adding 5% or 30% He to the Ar-10% CO_2 mixture has a slightly detrimental effect (Ar-10%CO_2 passed with S-3 wire whereas Ar-10%CO_2-5%He and Ar-10%CO_2-30%He ternary mixtures failed). The addition of 2%O_2 seemed to have a slightly detrimental effect when added to CO_2. However, added to form a quaternary gas mixture, O_2 had a beneficial effect (the upper two boxes).

Figure 3 shows the average ultimate tensile and yield strengths as a function of $\%CO_2$ in argon for both S-3 and S-6 electrodes. As can be seen, increasing the $\%CO_2$ slightly decreases both the ultimate and yield strengths, although all of the measured values were within the allowable range of CSA W48.4 weld properties. By comparing the values in Table 3 it can be seen that helium additions have little effect on the resulting tensile properties. Figure 4 shows the average ultimate tensile and yield strengths for the S-6 wire as a function of $\%CO_2$ including He additions as well.

Figure 5 shows the average charpy impact energy as a function of $\%CO_2$ in argon for both S-3 and S-6 electrodes. As can be seen, increasing the $\%CO_2$ decreases the impact toughness substantially for the S-6 wire but has little effect on the S-3 wire. However, it should be noted that these wires were tested in accordance with CSA W48.4 which means that they were tested at different temperatures (-20°C for S-3 and -30°C for S-6). Again, the effect of helium additions was seemingly random and of no significant effect, this is shown in Figure 6.

The validity of the IIW group index classification system was analyzed. Figure 7 shows the UTS and yield strength vs. group index for the S-6 wire. Figure 8 shows the Charpy vee-notch impact energy vs. group index for the S-6 wire, and Figure 9 includes the effect of helium.

Table 4 shows the chemical analyses for all of the welds made in this study. The oxygen and nitrogen analyses performed using drillings were discarded due to the high values and scatter. The results for silicon, carbon and oxygen are shown graphically in Figures 10-12 as a function of $\%CO_2$ in the argon shielding gas and in Figures 13-15 as a function of $\%O_2$ in the argon shielding gas. Figures 16-18 show these results as a function of IIW group index.

Although microstructures were obtained for all welds in this study, Figures 19-24 show a representative sampling from a wide diversity of different shielding gases. The greatest effect of shielding gas seems to be on the weld bead shape as is shown in the macrographs in Figures 25-30.

Discussion

Since this is an ongoing program, only a brief analysis of the experimental results will be given here.

The most important result is the discovery of significant amounts of porosity in multipass welds made with low oxidizing potential shielding gases.

The mechanism for this porosity formation is still unclear at present. One would normally expect that the higher oxidizing potential gases would have a higher propensity to form porosity, but this is obviously not the case here. An examination of Figures 28 and 29 show that the porosity appears to form along the fusion boundary, possibly due to the rejection of supersaturated elements such as carbon and oxygen. The porosity which was found near the centre of the weld is much larger, due to the accumulation of this smaller porosity. Thus, the removal of porosity should be affected by solidification rate and weld pool turbulence.

There are three possible mechanisms which would potentially explain why porosity forms with low oxygen concentrations in the shielding gas.

- Excess oxygen is absorbed by the weld pool due to the fact that oxygen will dissociate more readily at low concentrations. Monatomic oxygen absorbtion occurs more readily than diatomic oxygen, thus resulting in more oxygen being absorbed at lower overall concentrations of oxygen.

- SiO formation occurs rather than CO formation.

- CO forms at the fusion boundary, however, due to the fact that high argon shielding gases result in deep finger penetration, this gas is not allowed the opportunity to escape.

The experimentally determined weld oxygen contents at low shielding gas oxygen concentrations were eliminated because they were very high with large amounts of scatter. This was initially done because it was assumed that the scatter was due to the use of drillings rather than machined cylinders. However, if these values were actually accurate, then mechanism number one would appear valid. There is certainly one data point (an average of three readings) at low shielding gas oxygen concentrations which was very high even though machined slugs were used (Figure 15).

The welds performed with low oxidizing potential shielding gas should be re-evaluated to determine the weld metal oxygen content.

Thermodynamic calculations show that SiO is thermodynamically stable at molten weld pool temperatures. However, CO is even more stable. Ternary phase diagrams would have to be developed to show the applicability of this potential porosity formation mechanism. Previous results show that CO should not form with the weld pool silicon concentrations used in this study.

All of the welds which passed radiographic inspection and were porosity free met the weld property requirements in CSA W48.4 (with the exception of plate 21A which failed elongation slightly).

The slight variation in UTS and yield strength is not surprising since the overall composition of the weld metal does not vary substantially with shielding gas composition. It is more expected that slight differences in weld metal composition, especially the oxygen, will effect the impact toughness.

As can be seen from Figures 5 and 6, the amount of shielding gas CO_2 appears to significantly affect the impact toughness (for the S-6 electrode). However, there is no significant difference between the as deposited weld metal microstructures shown in Figures 19-24. A correlation between the amount of microstructural constituents such as bainite, acicular ferrite and proeutectoid ferrite and the impact toughness was attempted with no success. However, as can

be seen in the macrographs in Figures 25-30, the welds made with lower oxygen potential shielding gas has a greater proportion of reheated weld metal. The equiaxed ferrite resulting from reheating has a much higher impact toughness than the as deposited weld metal microstructures. Thus the effect of shield gas composition seems to have had a larger effect on the weld bead shape, and thus on the amount of reheated microstructures, than on the deposited microstructure itself.

The reason why the weld shape will have such a large effect on the amount of reheated weld metal can be explained by Figure 31. As is shown schematically, the HAZ shape and size are roughly equivalent for welds made with argon rich and CO_2 rich (referred to as "normal") shielding gases. However, the argon rich welds have a deep narrow finger penetration which results in a much larger area of HAZ. The "difference" in HAZ between these 2 types of shielding gases is indicated in the Figure.

Thus the influence of weld metal composition and number and distribution of inclusions on weld impact toughness could not be directly correlated with the experimental procedures used to date.

All of the welds met the charpy impact toughness requirements. However, it must be noted that these requirements are not very stringent. A great many other steel weldments are required to have higher impact toughness at lower temperatures and these results show that strict attention to the amount of weld metal oxygen may be important, but that the weld deposition sequence and bead shape may be even more important.

The IIW group index classification system was used to graph the experimental results of this study. There seems to be a good correlation between the group index and amount of weld metal oxygen at higher group index levels, however, the amount of weld metal oxygen at lower levels must still be investigated. The correlation with weld metal carbon and silicon appears to have too much scatter. The correlation with impact toughness does not appear to be very good, however, the effect of weld pool shape must be considered.

A more detailed analysis and discussion of the results will be performed in future work.

Conclusions

This is the first phase of a program to determine acceptable ranges of shielding gas - filler metal - base metal combinations. The present report discusses previous results and the results of the current experimental program.

1) The ISO has adopted a classification for filler metals and a different classification system for shielding gases. The two classification systems are not linked however.

2) Previous experimental results on the effect of shielding gas composition on weld metal composition and properties are contradictory and contain a great deal of scatter.

3) Previous thermodynamic gas-metal reaction theories are contradictory and insufficient to provide a basis for developing a predictive analysis for selecting acceptable shielding gas - filler metal - base metal combinations.

4) It was found in the present investigation that low oxidizing potential shielding gases can cause porosity in multipass welds. This is a significant new discovery never previously published.

5) All of the weldments made with shielding gases which did not produce porosity met the CSA W48.4 weld metal property requirements (with one exception).

6) The shielding gas composition significantly affects weld bead shape which, in turn, affects the amount of reheated weld metal microstructure which affects the impact toughness. Although high shield gas $C0_2$ levels result in lower impact toughness, in this study this is more likely due to the effect of bead shape than to the number and distribution of oxides.

7) CSA W48.4 should be modified to restrict the use of low oxidizing potential shielding gases in multipass applications on mild steel.

8) Future work should develop a predictive ability to determine acceptable shielding gas - filler metal - base metal combinations

Proposed Modifications to CSA W48.4

Based on the results of this study, the use of low oxidizing potential shielding gases in multipass applications should be restricted. Since the precise ranges where porosity occurs has not been established yet, the following conservative approach is recommended (whether or not to include the S-2 wire into this statement should be seriously considered).

Table 2 in CSA standard W48.4 should immediately be changed to state:

† The specified 100% CO_2 shielding gas may be replaced by a binary, ternary, or quaternary mixture of Ar-He-O_2-CO_2 with the following restrictions:

For multipass applications, gas mixtures shall not contain less than 10% O_2 or CO_2. Helium may replace argon in amounts of up to 30% provided that there is as least 25% CO_2 in multipass applications. Multipass applications using a shielding gas outside of these recommended ranges shall be requalified.

Proposed Future Work

A thorough analysis of previous investigations has discovered a great deal of contradictory experimental results and thermodynamic gas-metal analyses. A comparison of experimental results on nominally identical welds found average differences in silicon content of over 100%. Theoretical analyses have found absorption temperatures ranging from 1600°C to 2700°C and dissociation values from zero to 85%.

The present experimental results have determined that porosity can occur in multipass applications on mild steel with low oxidizing potential shielding gases but has not delineated these ranges.

Even though it is well recognized that a standard should link the shielding gas composition to the filler metal composition, this has never been performed.

In light of the above, WIC proposes a three step program to determine acceptable ranges of shielding gas - filler metal - base metal compositions:

1) The current experimental program must be broadened to include higher strength steels and a broader range of electrode compositions. The effect of elemental transfer will be much more important in these steels in order to obtain the proper amount of oxides and strengthening elements. Thus it is imperative to develop the capability of selecting appropriate shielding gas compositions for these steels.

   Additionally, the precise range of acceptable shielding gases to prevent porosity should be delineated for both these steels and the mild steel used in the present phase of the program. The existing WIC computerized gas mixing system can be used to accurately and economically examine a wide range of gas mixtures.

2) An experimental apparatus should be constructed to determine the amount of elemental transfer occurring at the electrode tip, during droplet transfer across the arc plasma, and in the weld pool. This apparatus could be based on the one built by Grong and Christensen. Additionally, the WIC Arc Physics Laboratory's ability to determine the arc plasma composition and temperature should be used to determine the contribution of elemental vaporization to elemental losses as well as determine the effect of helium and other elements on arc plasma temperature.

   Depending on available funding, the influence of shielding gas and filler metal composition as well as welding parameters on fume formation (and the effect of loss of elements through fume) should be determined. The existing WIC fume generation chamber can be used to determine the fume generation rates and fume composition.

3) A thermodynamic analysis should be conducted which uses known weld pool temperatures rather than trying to calculate the effective reaction temperature based on elemental transfer values. A two stage mechanism of weld pool absorption should be used based on using the cathode boundary layer temperature to determine the amount of dissociation and an absorption temperature based on the actual temperature of the weld pool. The incorporation of the influence of monatomic oxygen absorption will explain the fact that oxygen absorption is a linear function of oxygen in the shielding gas.

Percent dissociation as a function of BOTH pressure and temperature needs to be derived and incorporated into this model. Most previous theories neglected to calculate the increased amount of dissociation at lower than atmospheric pressures. Previous dissociation curves assumed 100% CO_2 or O_2. In fact if there is only 2% O_2, then there will be more dissociation at the same temperature than had there been 100% O_2 (this fact is based on LaChartier's principle - if there are fewer oxygen molecules, they will want to take up more volume by dissociating).

Solidification kinetics should then be used to determine the range of compositions which result in porosity formation. The Shiel equations can be used to determine the effect of solute rejection as a function of solidification rate thereby increasing the amount of oxygen (note that the effective reaction temperature should not in fact change as a function of welding speed -- solidification mechanisms should be taken into consideration to account for the change in elemental transfer).

This gas-metal reaction model will be developed with the explicit desire to have a predictive analysis tool to determine acceptable shielding gas - filler metal - base metal combinations. The model will not be developed merely for the sake of science, but will be used to develop a set of standards linking acceptable shielding gas compositions to filler metal and base metal compositions.

References

1) Gilde W. Zur Thermodynamik der Schutzgasschweissung mit Kohlensaure, vol. 6 #6, June 1956, pp 164-167.

2) Pollard, B., Milner, D.R. "Gas Metal Reactions in $C0_2$ Arc Welding". Journal of the Iron and Steel Institute, April 1971, pp. 291-300.

3) Coe, F.R., Moreton, J. "The Chemistry of Oxygen in Gas-Shielded Welding of Steel". TWI Doc. 95/1979, July 1975.

4) Heile, R.F., Hill, D.C. "Particulate Fume Generation in Arc Welding Processes", Welding Research (Supp.to The Welding Journal), July 1975, pp 201-208.

5) Svecinskij, V.G., Rimskij, S.T. "The Effect of Gas Composition upon Material Transfer during Mag-Welding", ZIS-Mitteilungen, Vol 24, No. 6, June 1982, pp 601-609.

6) Grong, O., Christensen, N, "Factors Controlling MIG Weld Metal Chemistry", Scandinavian Journal of Metallurgy" 4 (1983) 155-165.

7) Block-Bolten, A., Eagar, T.W., "Metal Vaporization from Welds Pools", Met. Trans. Vol. 15B, Sept. 1984, pp. 461-469.1

8) Block-Bolten, A., Eagar, T.W., "Selective Evaporation of Metal from Weld Pools", Trends in Welding Research in the U.S., ASM, Metals Park, Ohio, 1982, pp. 53-73

9) Meyendorf, N., "Metal Gas Reactions in Gas-Shielded Arc Welding", ZIS-Mitteilungen 1978 29 (8), Welding International 1988, No. 7, pp 653-657.

10) Quigley, M.B.C., "Physics of the Welding Arc", Welding & Metal Fabrication, Dec. 1977, pp 619-626.

11) Gedeon S.A. "Hydrogen Assisted Cracking in High Strength Steel Welds" Doctoral Thesis, Massachusetts Institute of Technology, June, 1987.

12) Dinulescu, H.A., Pfender, E., "Analysis of the Anode Boundary Layer of High Intensity Arcs", Journal of Applied Physics, 51 (6), June 1980, pp. 205s-211s.

13) S.A. Gedeon and T.W. Eagar, "Thermochemical Analysis of Hydrogen Absorption in Welding", Welding Journal, July 1990, pp 264s-271s.

14) "Recommendations for the Standardization of Solid Steel Electrodes for Gas Shielded Bare Wire Arc Welding of Structural Steel in the Tensile Range 35-52 kg/mm^2 (Minimum Values)", IIW Doc. XII-B-75-70, 1970.

15) Dr. Ing. W.E.W. Ruckdeschel, "Experimental Studies to Establish the Oxidation Potential or MIG Shielding Gases for Gases". IIW Doc. XII-B-177-75.

16) Shackleton, D.N., Ruckdeschel, W.E.W., "The Effect of Gas Mixture in MIG Welding of Ferritic Steel on Oxygen Transfer and Weld Metal Impact Values".

17) Shackleton, D.N., "Contribution to Experimental Studies to Establish the Oxidation Potential of MIG Shielding Gases for Steels", IIW Doc. XII-B-171-74.

18) Hans-Ulrich Pomaska, "Determination of the Oxidation Potential of Shielding Gas Mixtures and $C0_2$ with a view to Classifying Gas-Wire Combinations", IIW Doc. XII-B-190-75.

19) Konkoly, Tibor, "The Influence of the Welding Conditions on the Notch Toughness of MIG-$C0_2$ Weld Metal". IIW Doc. XII-B-66-70.

20) A.A. Smith, "Classification of Shielding Gases used in the gas shielded arc welding of ferrous metals - on the basis of their oxidation potential", IIW Doc. XII-669-77.

21) Dr. A.A. Smith, "Classification of Shielding Gases used in the Gas Shielded Arc Welding of Ferrous Metals - on the basis of their Oxidation Potential", Welding in the World, Vol. 16. No. 1/2/78.

22) R.E. Francis, J.E. Jones & D.L. Olson, "Effect of Shielding Gas Oxygen Activity on Weld Metal Microstructure of GMA Welded Microalloyed HSLA Steel", Welding Journal, Nov. 1990 pp 408s-415s.

23) D.N. Shackleton, A.A. Smith, "Standardization of Shielding Gas Mixtures for MIG/MAG Welding", IIW Doc. XII-D-23-84.

TABLE 1

GMAW Electrode Compositions used in this Study

Class & Heat No.	Analysis	C	Mn	P	S	Si	Cu	O	N
ER70S-6	Supplied	.08	1.51	.014	.014	.92	.010	-	-
086462	External	.09	1.40	.08	.014	.92	.07	202ppm	45ppm
ER70S-3	Supplied	.10	1.080	.015	.014	.530	.040	-	-
182955	External	.11	1.00	.08	.014	.54	.10	182ppm	37ppm

TABLE 2

Steel Composition used in this Study
BASE PLATE: CSA G40.21 Gr. 44W

HT #400053	
	%
C	0.16
Mn	1.37
P	.006
S	.003
Si	0.25
Cu	0.25
Ni	.009
Cr	.015
Mo	.007
V	.003
Cb	.002
Nb	.002

TABLE 3: TEST MATRIX AND MECHANICAL TEST RESULTS

Weld #	Gas Composition				Wire Class	Amps	Volts	Trav. Speed	Heat Input	Avg. CVN	Avg. UTS	Avg YS	Avg. Elon	X-Ray
	Ar	CO_2	O_2	He										
3	95	5	-	-	S-6	320.5	29.5	13 ipm	43.6					Fail
4	90	10	-	-	S-6	329	30	14 ipm	42.3	82.5J	582	484	24.3	Pass
26	85	10	-	5	S-6	333.9	29.5	15 ipm	39.4	71.7J	545	440	25.67	Pass
10	60	10	-	30	S-6	339	33	16 ipm	42	100.7J	589	477	27.5	½ pl. Fail
6	85	15	-	-	S-6	334	31.5	15 ipm	42	108.7J	578	469	27.8	Pass
20	75	25	-	-	S-6	297.4	29	14 ipm	37	67.3J	595	477	25.5	Pass
23	70	25	-	5	S-6	312.2	31.5	14 ipm	42.1	54.7J	569	429	26.3	Pass
24	45	25	-	30	S-6	297.5	32	14 ipm	40.8	69.7J	577	462	27.7	Pass
22	50	50	-	-	S-6	293.3	32	14 ipm	40.2	46.3J	563	447	26	Pass
1	-	100	-	-	S-6	280	28	12 ipm	39.2	43.3J	567	458	26.9	Pass
17	99.5	-	.5	-	S-6	320	29.5	14 ipm	40.5					Fail
7	98	-	2	-	S-6	352	28	15 ipm	39.4					Fail
33A	98	-	2	-	S-6	361	28	15 ipm	40.4					Fail
28	93	-	2	5	S-6	361	29.5	15 ipm	42.6					Fail
9	68	-	2	30	S-6	348	30	15 ipm	41.8					Fail
14	88	10	2	-	S-6	343	31	15 ipm	42.5	86J	575	471	28.3	½ pl. Fail
25	83	10	2	5	S-6	311.9	30	14 ipm	40.1	63.3J	581	470	26.3	Pass

TABLE 3: TEST MATRIX AND MECHANICAL TEST RESULTS (Cont'd)

Weld #	Gas Composition				Wire Class	Amps	Volts	Trav. Speed	Heat Input	Avg. CVN	Avg. UTS	Avg YS	Avg. Elon	X-Ray
	Ar	CO_2	0_2	He										
13	58	10	2	30	S-6	336	34	17 ipm	40.3	131.3J	569	469	27.2	Pass
18	95	-	5	-	S-6	323	27.5	13 ipm	41					Fail
19	90	-	10	-	S-6	314	28	12 ipm	44	129.3J	542	447	28	Pass
5	90	10	-	-	S-3	335	30	14 ipm	43.1	118J	545	449	27.8	Pass
27	85	10	-	5	S-3	339	29.5	15 ipm	40					Fail
11	60	10	-	30	S-3	343	33	16 ipm	42.4					Fail
21	75	25	-	-	S-3	298.2	29.5	14 ipm	37.7					Fail
21A	75	25	-	-	S-3	307	30	13 ipm	42.5	127J	541	439	22.3	Pass
2	-	100	-	-	S-3	280	28	12 ipm	39.2	117J	514	420	27.8	Pass
16	99.5	-	.5	-	S-3	363.8	31	16 ipm	42.3					-
8	98	-	2	-	S-3	351	28	15 ipm	39.3					Fail
33	90	-	10	-	S-3	327	28.5	13 ipm	43	97J	516	426	20.3 *	Pass
15	88	10	2	-	S-3	340.3	31	15 ipm	42.2	113J	542	444	27.4	½ pl. Fail
12	58	10	2	30	S-3	349	34	17 ipm	41.9	140J	524	427	27.4	Pass

*Does not meet spec.

Table 4: Weld Metal Composition vs. Gas Composition

Plate #	Gas Composition			Metal Composition					
	O2	CO2	He	O	C	Si	Mn	H2	N
	Percent	Percent	Percent	ppm	Percent	Percent	Percent	mL/100g	ppm
S6 Wire									
3		5		N/A	0.076	0.86	1.4	5.8	N/A
4		10		289.3	0.084	0.80	1.2	3.9	49
26		10	5	249.0	0.090	0.77	1.2	N/A	43
10		10	30	N/A	0.091	0.73	1.2	N/A	N/A
6		15		301.0	0.097	0.75	1.2	N/A	55
20		25		497.0	0.094	0.75	1.2	N/A	64
23		25	5	468.0	0.098	0.61	1.1	N/A	53
24		25	30	509.0	0.087	0.71	1.1	N/A	54
22		50		620.0	0.088	0.68	1.1	N/A	61
1		100		718.7	0.096	0.77	1.2	2.6	51
17	0.5			N/A	0.076	0.82	1.3	N/A	N/A
7	2			175.0	0.069	0.84	1.3	3.9	46
33A	2			N/A	N/A	N/A	N/A	N/A	N/A
28	2		5	N/A	0.082	0.79	1.2	N/A	N/A
9	2		30	N/A	0.072	0.81	1.3	N/A	N/A
14	2	10		N/A	0.088	0.73	1.1	N/A	N/A
25	2	10	5	323.0	0.079	0.77	1.2	N/A	45
13	2	10	30	266.3	0.089	0.69	1.1	5.9	52
18	5			N/A	0.070	0.76	1.2	N/A	N/A
19	10			416.7	0.074	0.66	1.1	4.5	53
S3 Wire									
5		10		372.0	0.110	0.43	0.87	5.2	44
27		10	5	337.0	0.110	0.40	0.84	N/A	43
11		10	30	N/A	0.120	0.39	0.82	N/A	N/A
21		25		581.0	0.098	0.48	0.85	N/A	48
21A		25		504.0	0.100	0.39	0.86	N/A	48
2		100		713.3	0.098	0.41	0.87	N/A	44
16	0.5			N/A	0.092	0.51	1.00	N/A	N/A
8	2			N/A	0.088	0.47	0.95	N/A	N/A
33	2			605.0	0.084	0.31	0.69	N/A	54
15	2	10		358.3	0.110	0.40	0.88	N/A	47
12	2	10	30	395.0	0.100	0.35	0.73	N/A	54

The compositions of the following elements do not change significantly within welds created with the same wire

S6 Wire:
0.014%S, 0.014%P, <0.005Al, 0.018%Cr, 0.020%Ni, <0.010%Nb, 0.0066%V, 0.12%Cu
0.0025%B, 0.0016%Ni, <0.010%W, 0.0032%Sn, 0.012%Co, 0.0050%Zr, <0.005%Rb

S3 Wire
0.014%S, 0.014%P, <0.005Al, 0.045%Cr, 0.032%Ni, <0.010%Nb, 0.0011%V, 0.12%Cu
0.0007%B, 0.0013%Ni, <0.010%W, 0.0040%Sn, 0.012%Co, 0.0040%Zr, <0.005%Rb

Figure 1: Weld Quality vs. Percent Oxygen

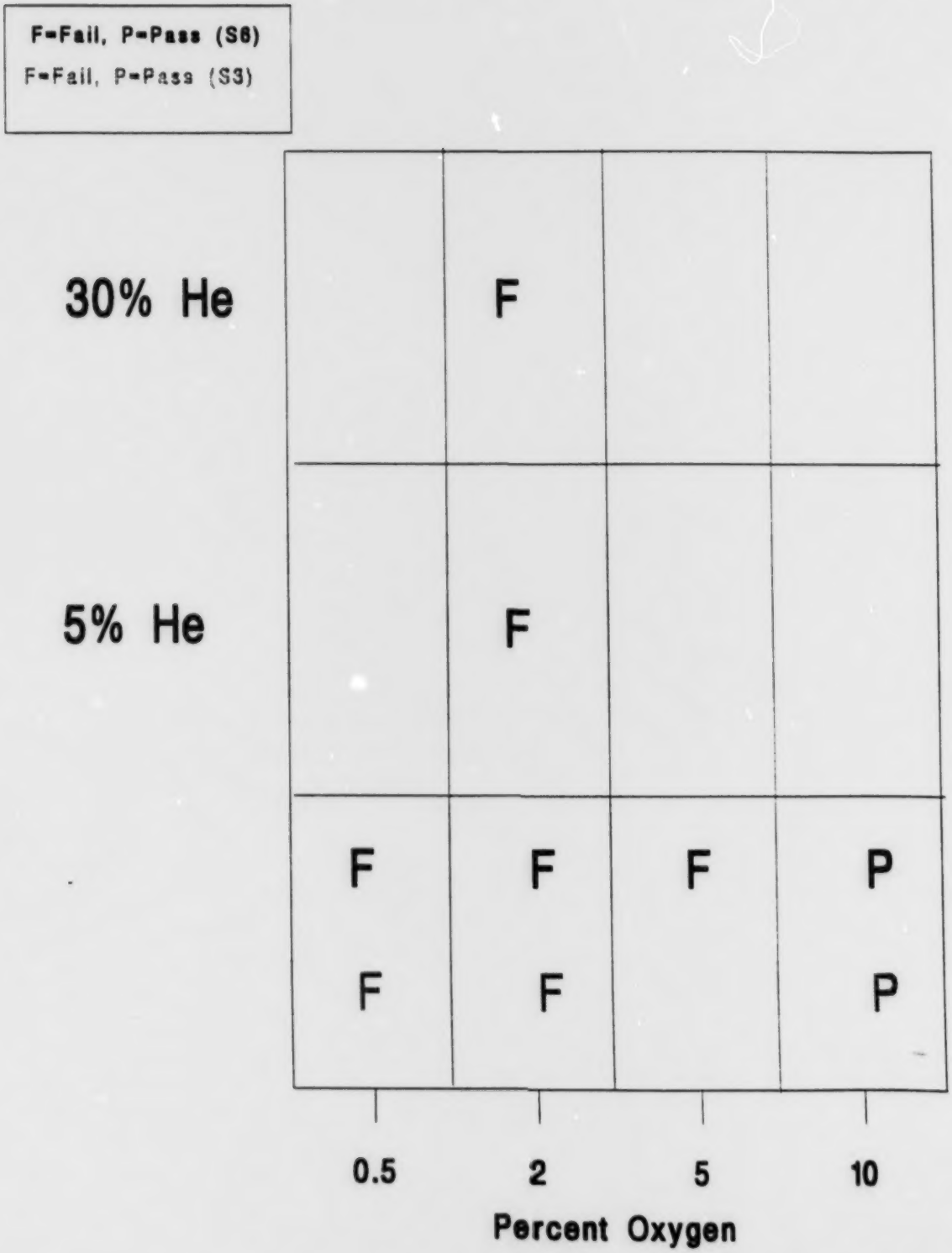

Figure 2: Weld Quality vs. Percent Carbon Dioxide

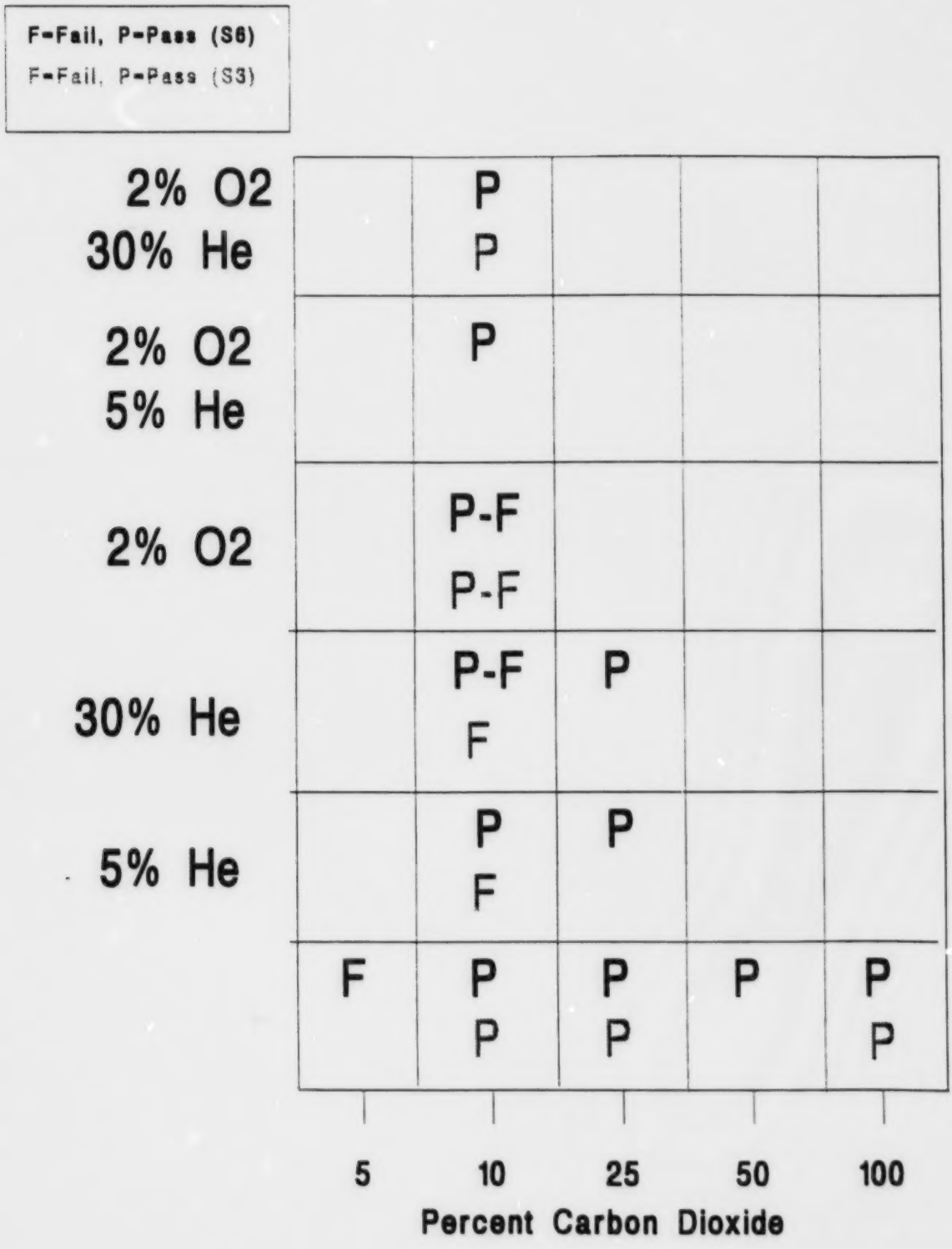

Figure 3: UTS and Yield Strength vs. % CO2

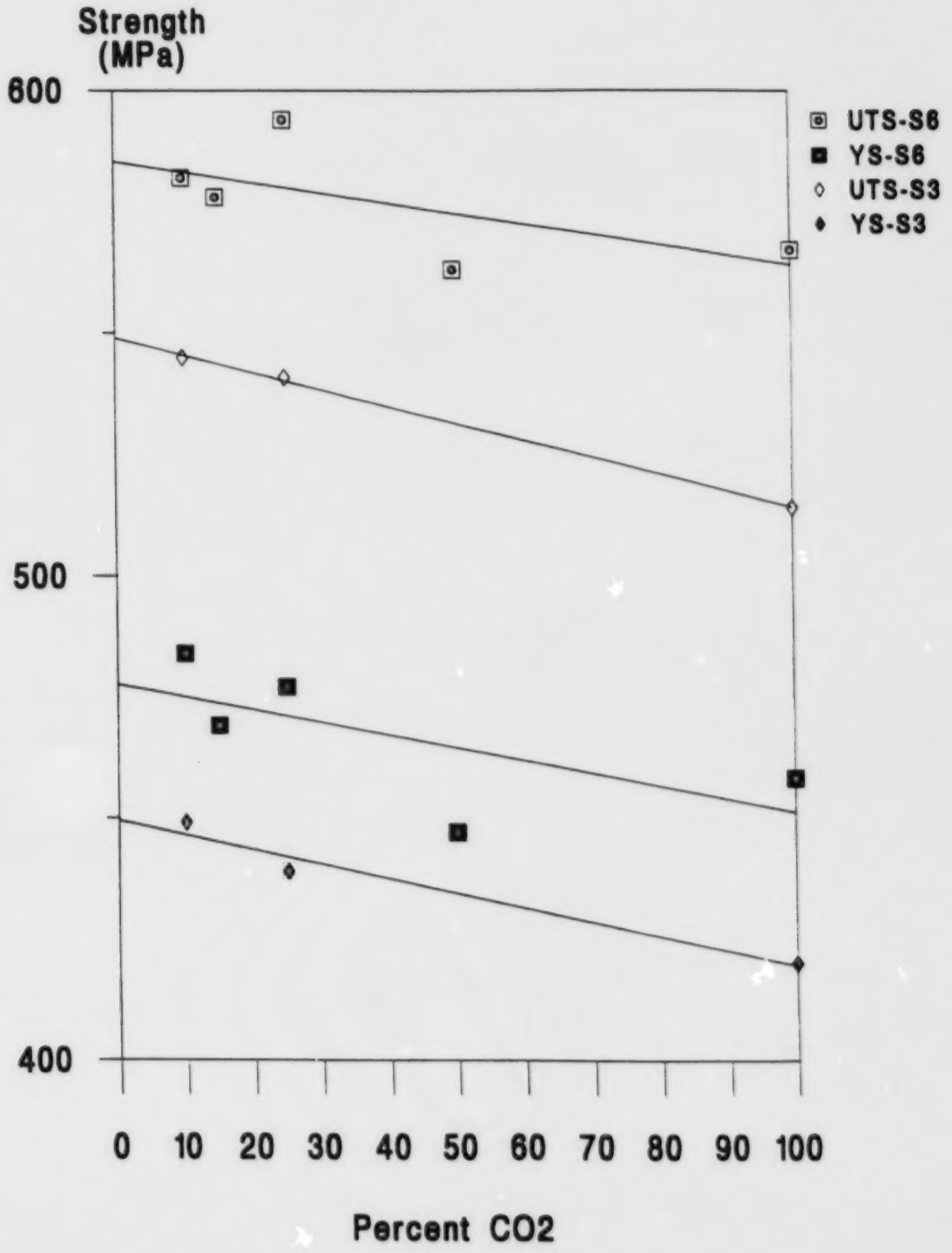

Figure 4: UTS and Yield Strength vs. % CO2 (S-6 Wire Only)

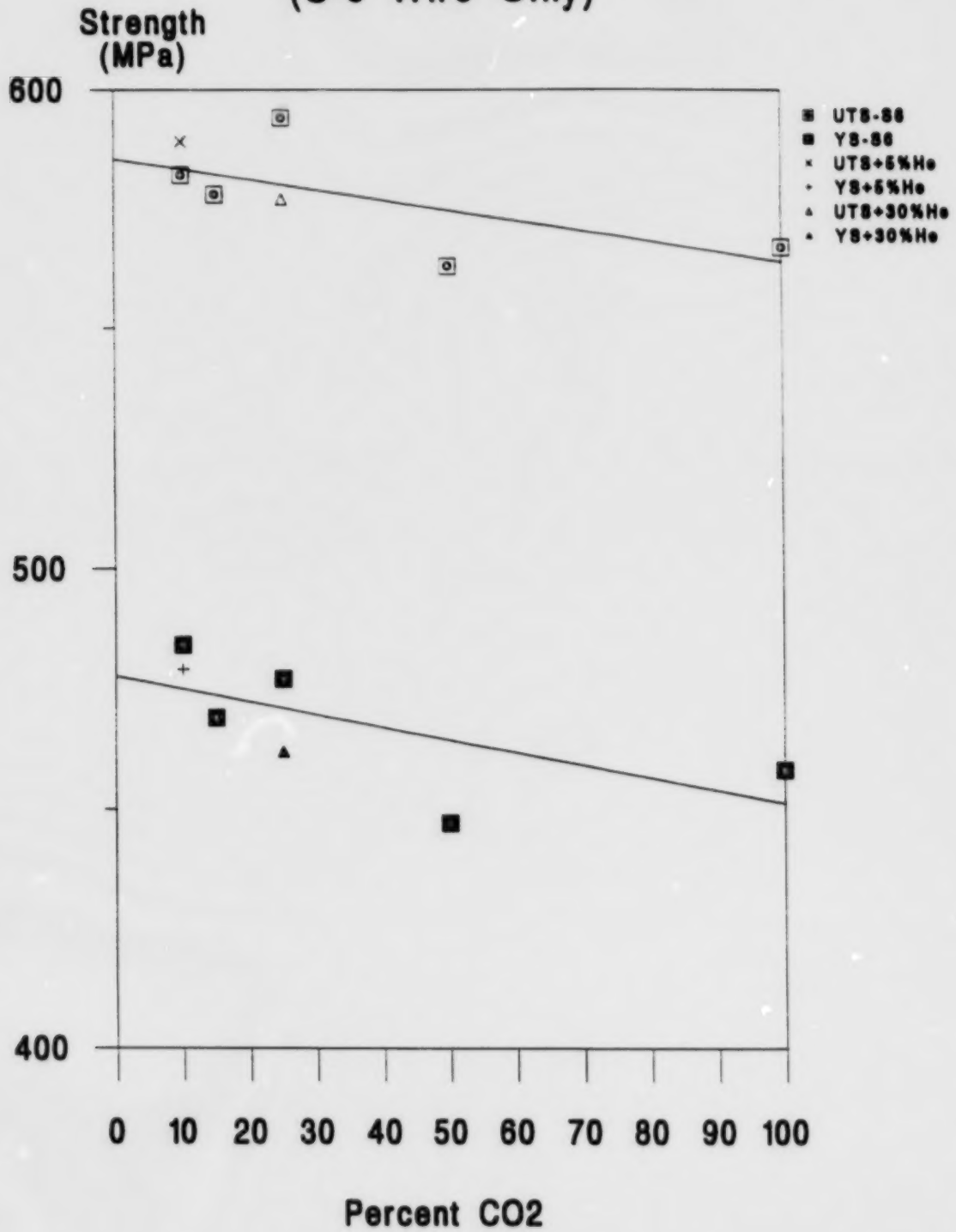

Figure 5: Charpy Impact Energies vs. % CO2

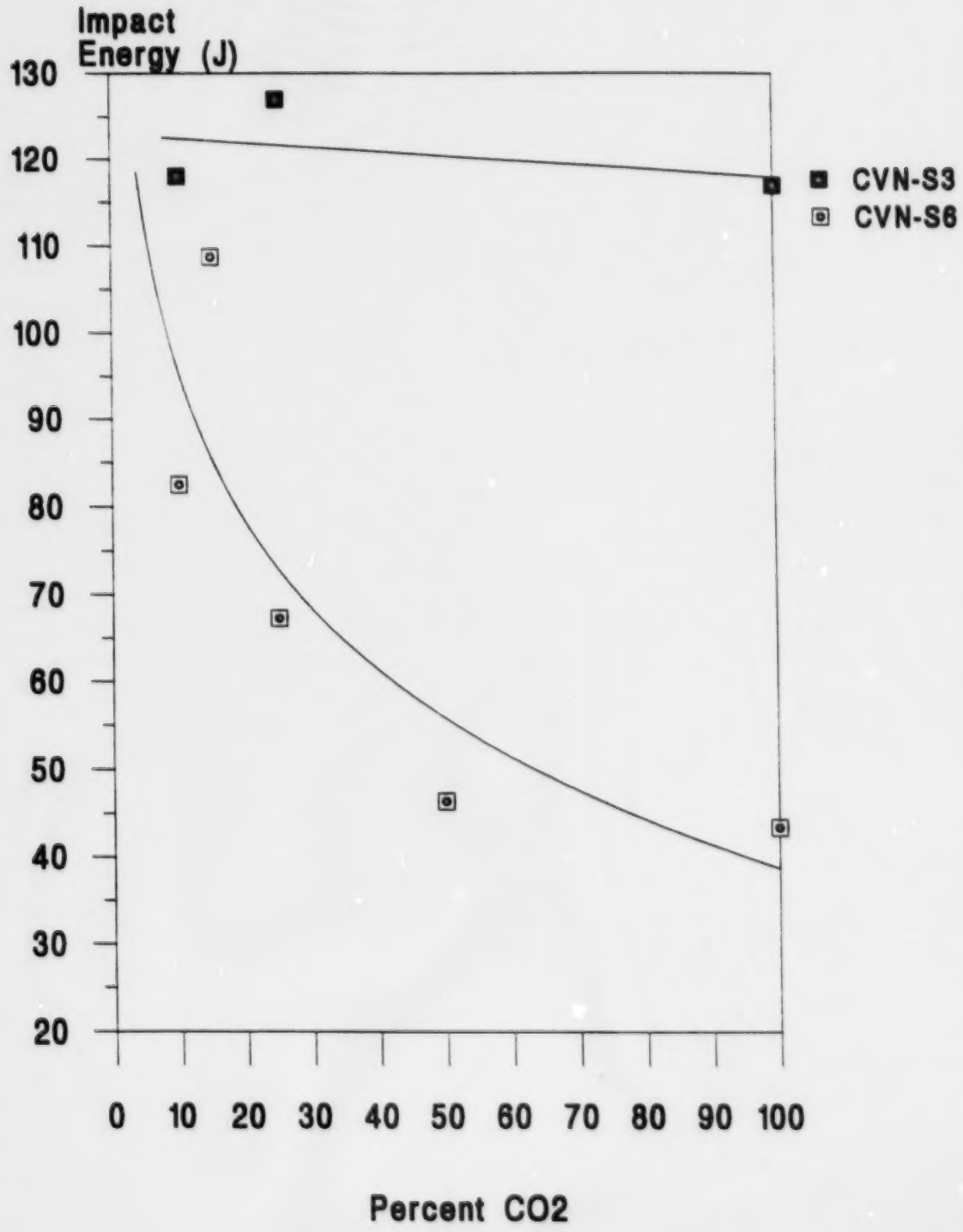

Figure 6: Charpy Impact Energies vs. % CO2
(S-6 Wire only)

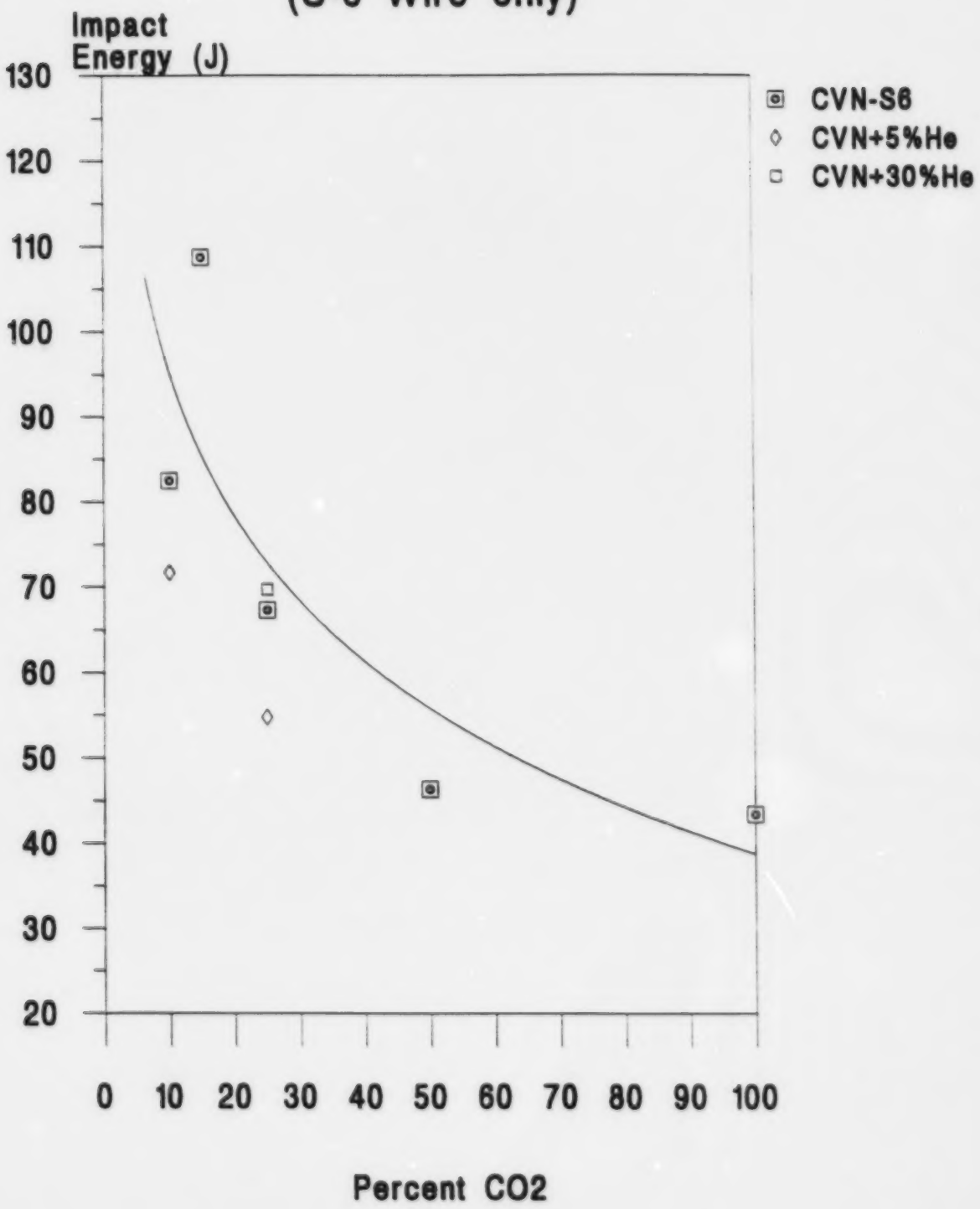

Figure 7: UTS and Yield Strength vs. Group Index (GI=%O2+1/2%CO2)

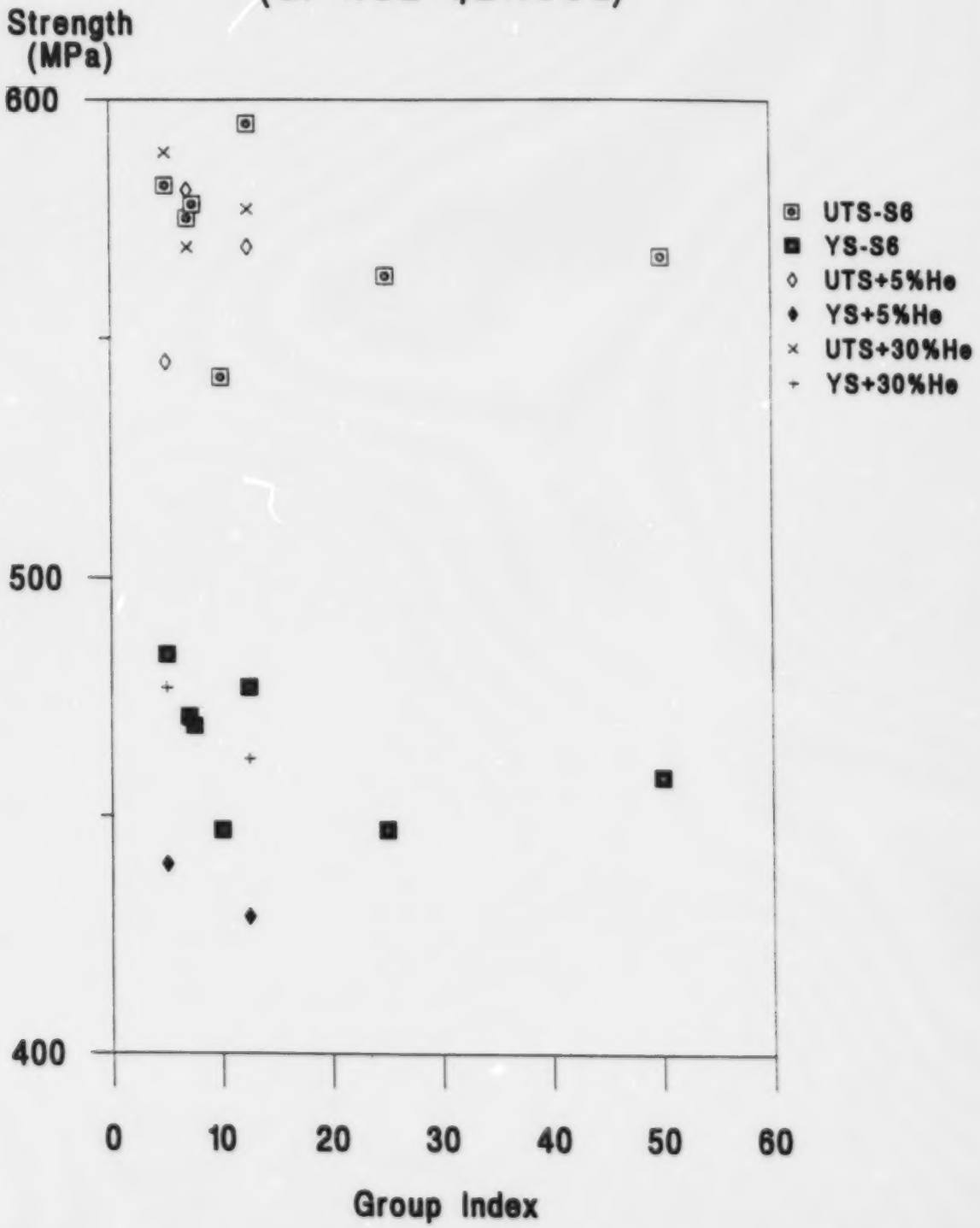

Figure 8: Charpy Impact Energies vs. Group Index (G.I.= %O2+1/2%CO2)

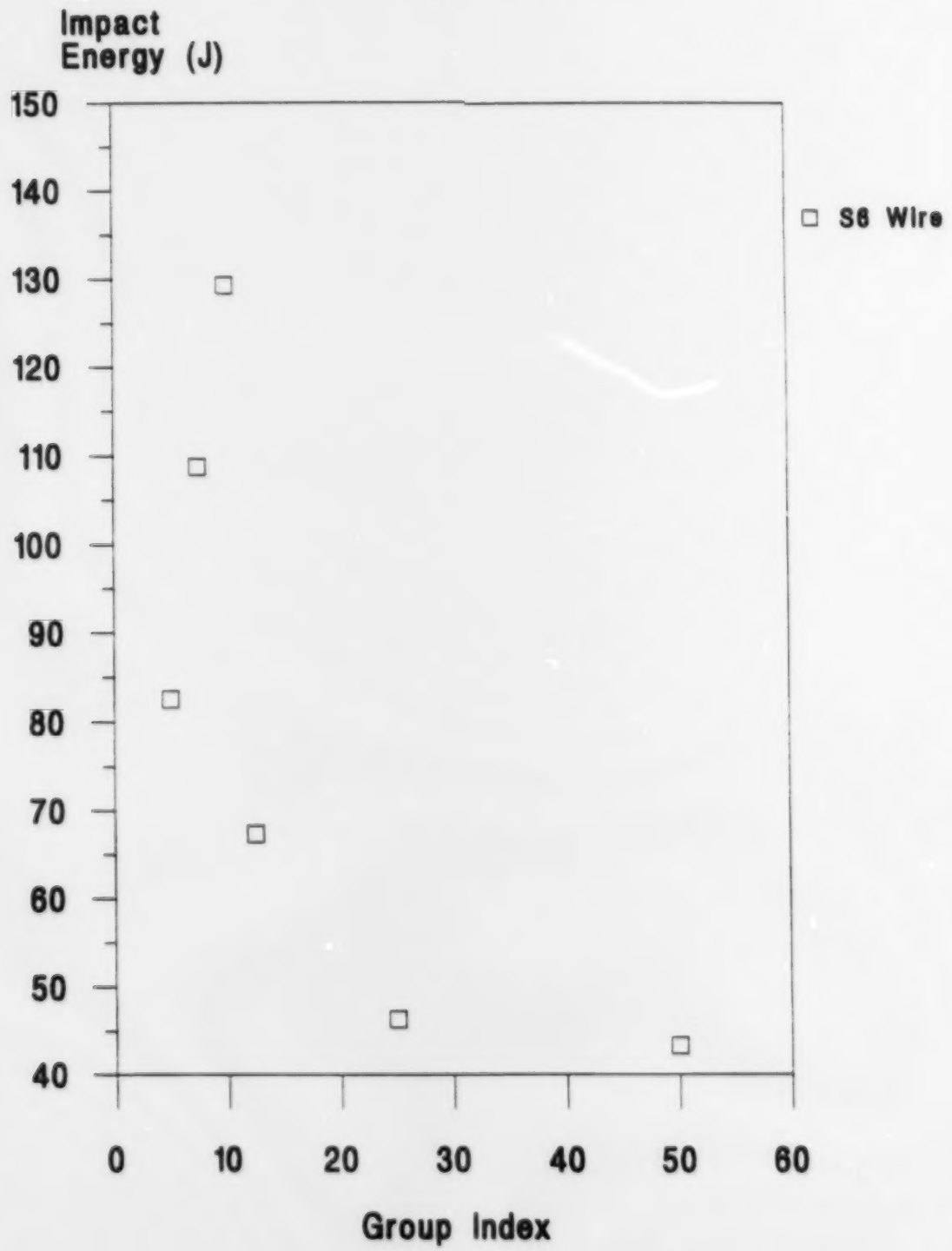

Figure 9: Charpy Impact Energies vs. Group Index (G.I.= %O2+1/2%CO2)

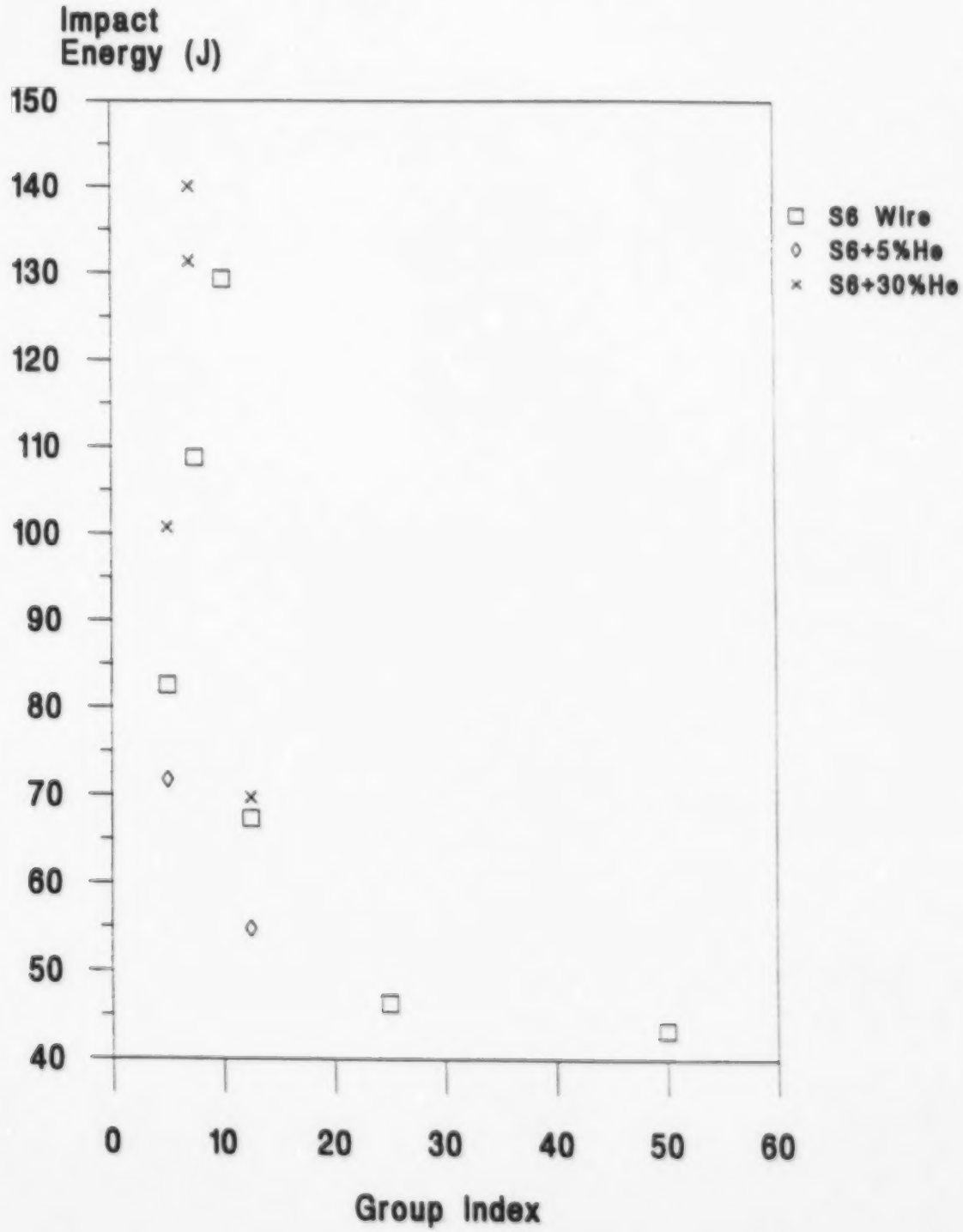

Figure 10: Weld Metal Carbon vs. Shield Gas CO2

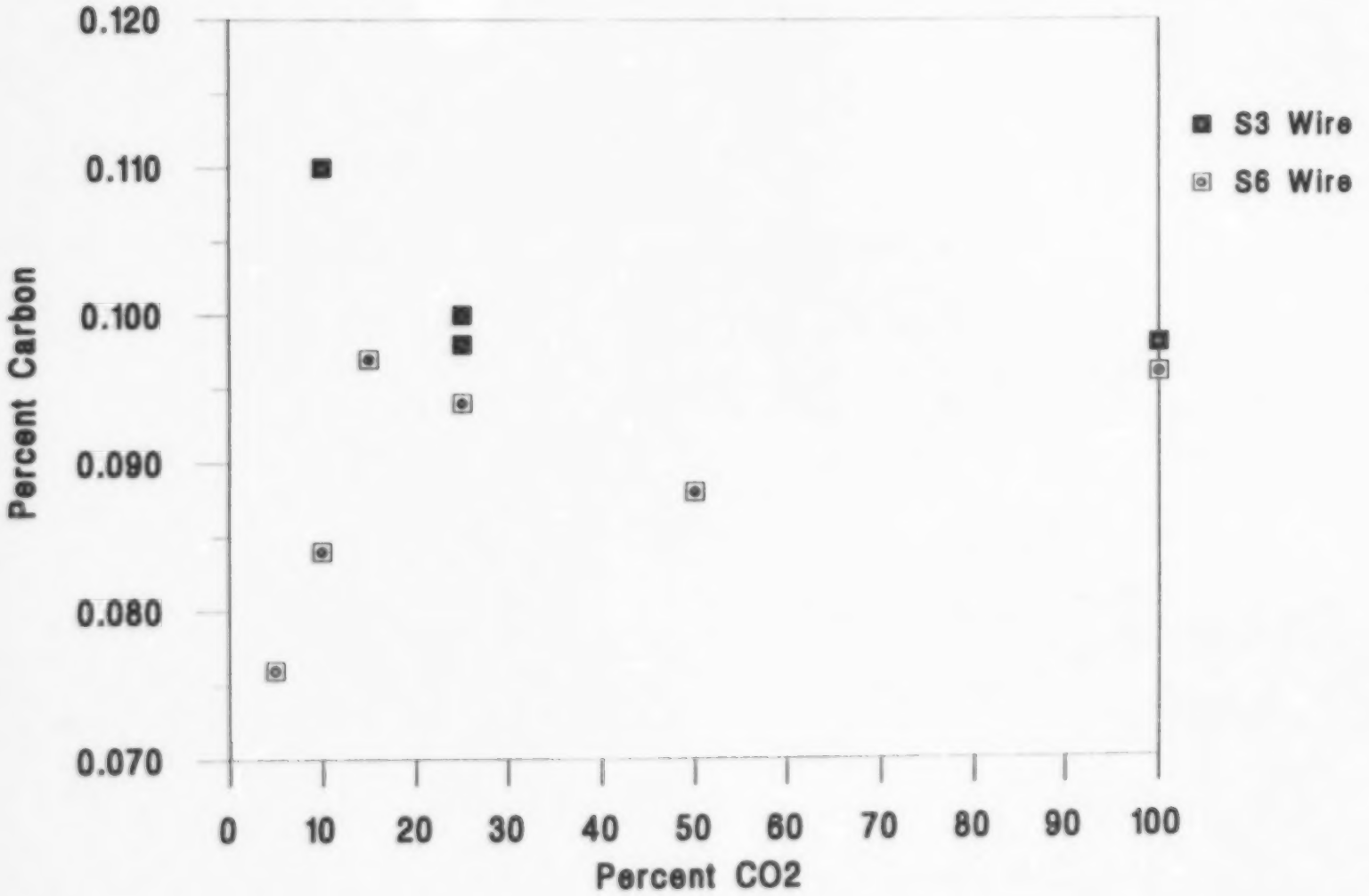

Figure 11: Weld Metal Silicon vs. Shield Gas CO2

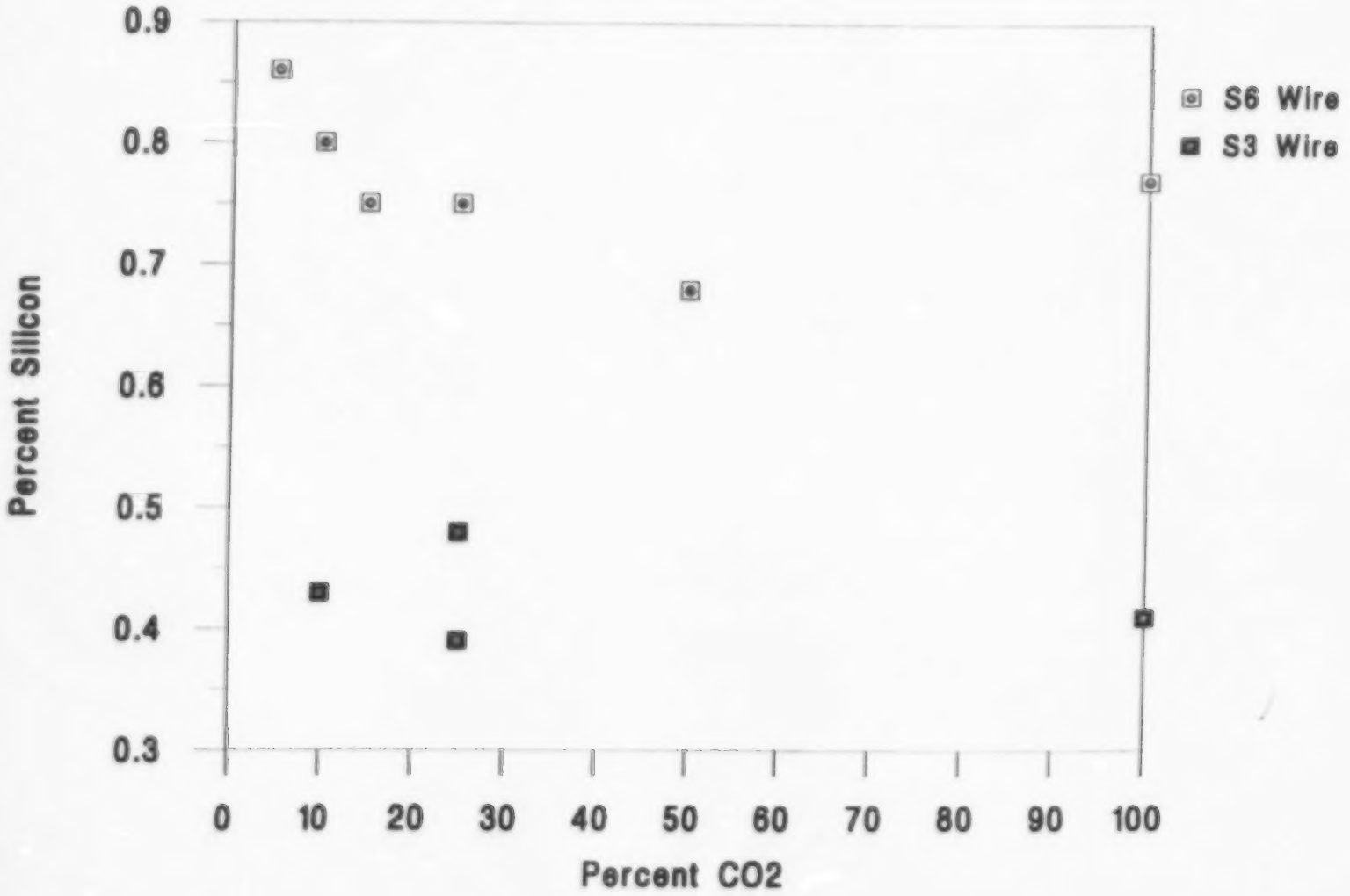

Figure 12: Weld Metal Oxygen vs. Shield Gas CO2

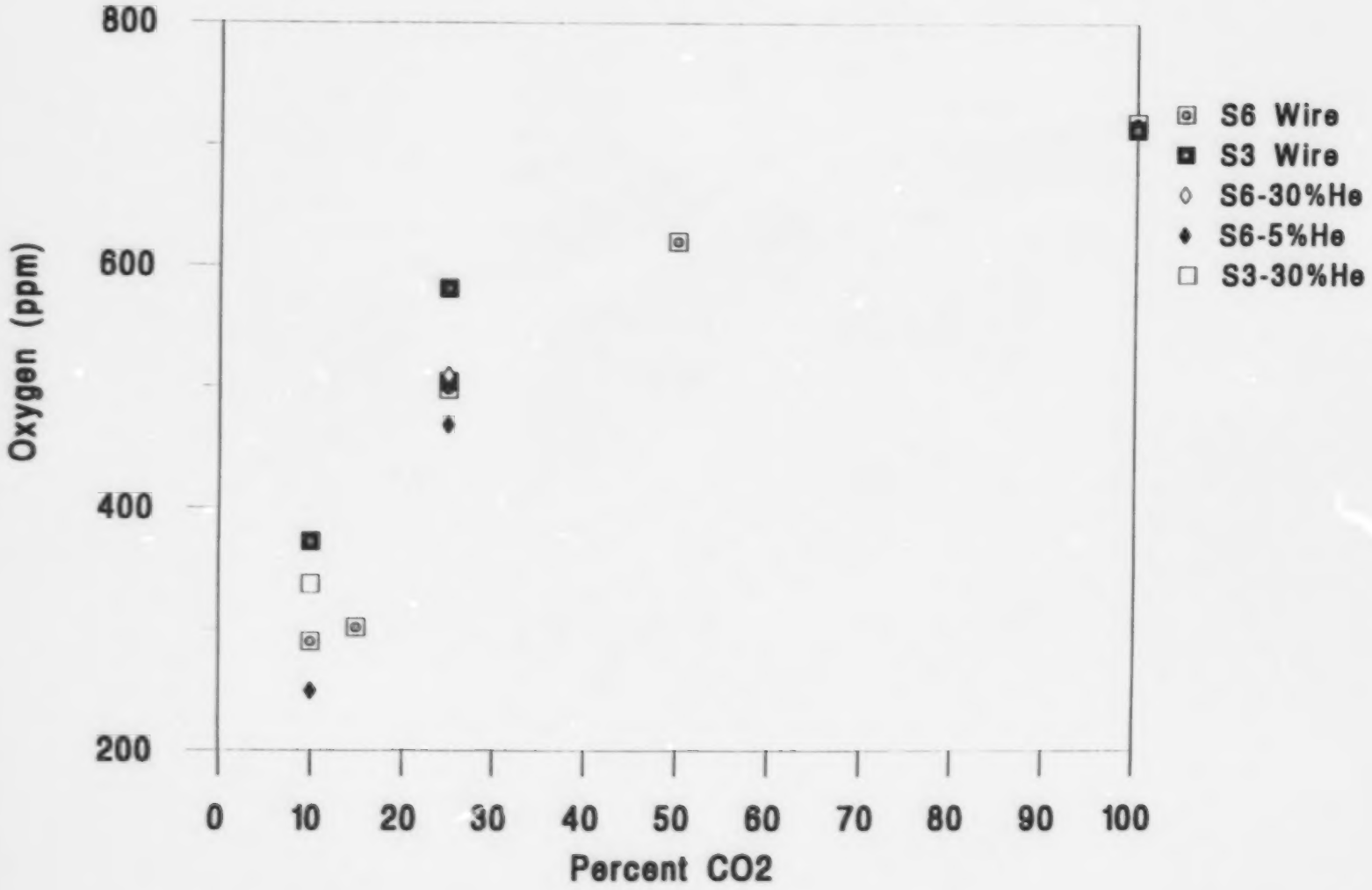

Figure 13: Weld Metal Carbon vs. Shield Gas Oxygen

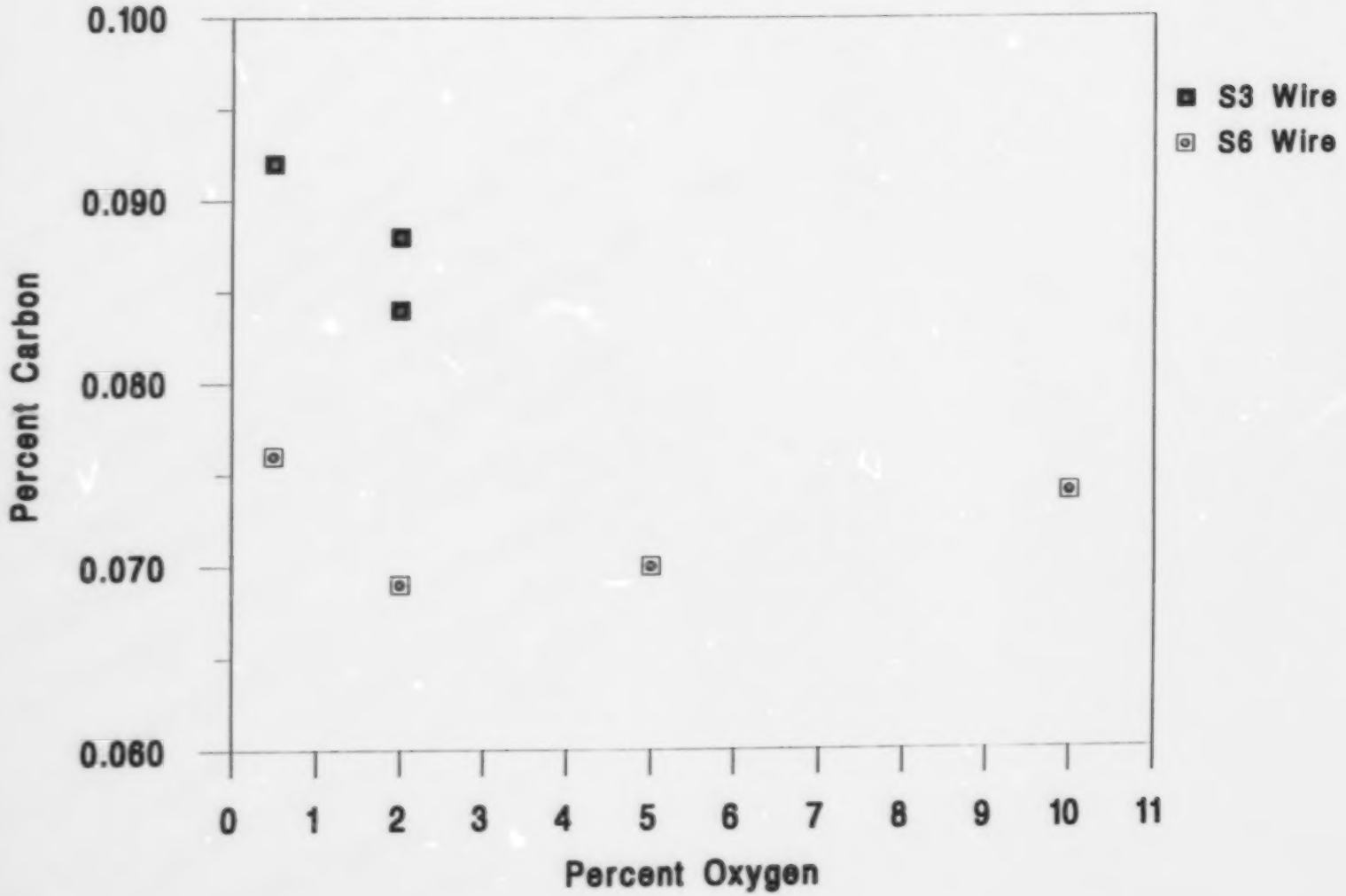

Figure 14: Weld Metal Silicon vs. Shield Gas Oxygen

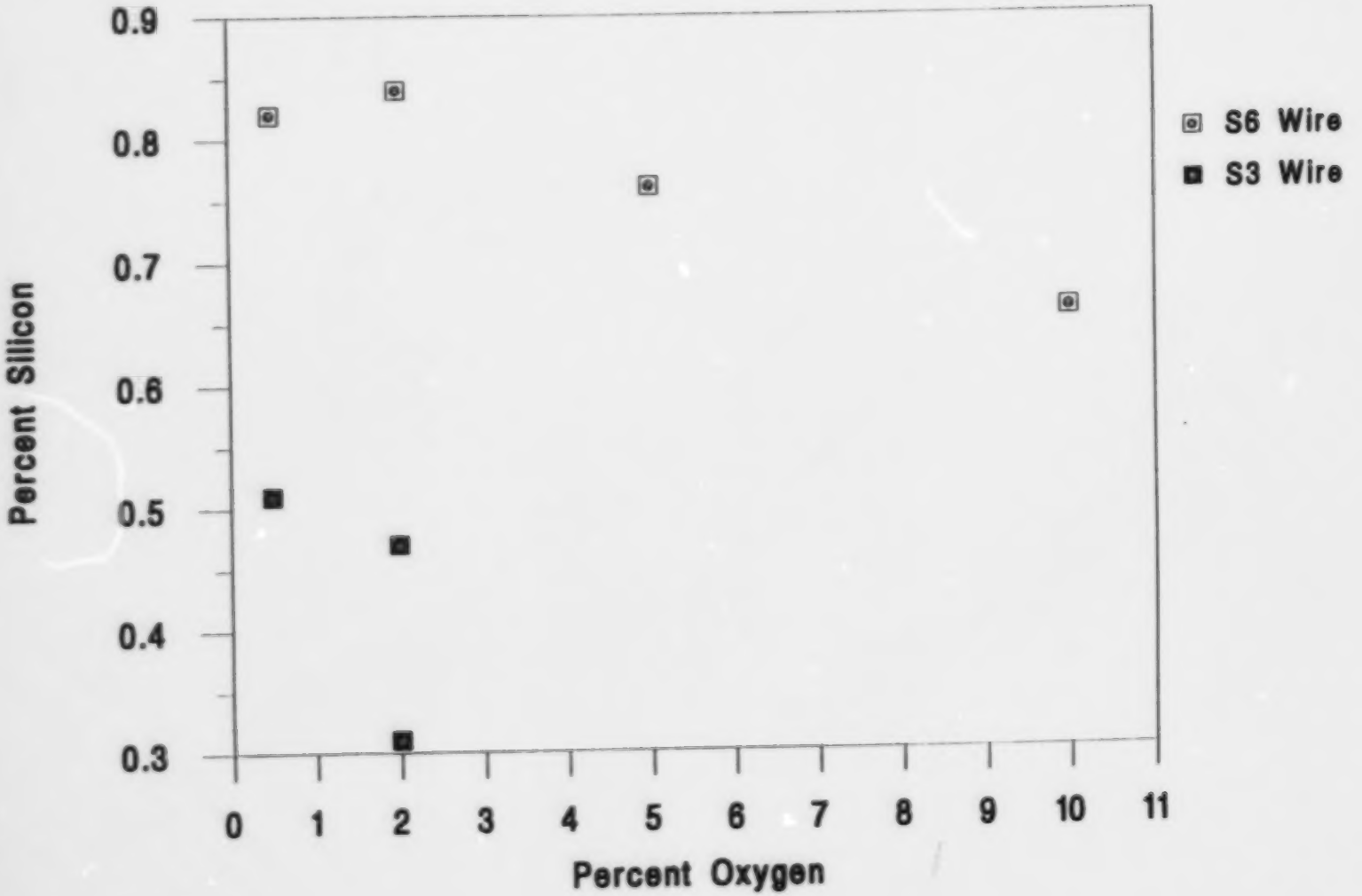

Figure 15: Weld Metal Oxygen vs. Shield Gas Oxygen

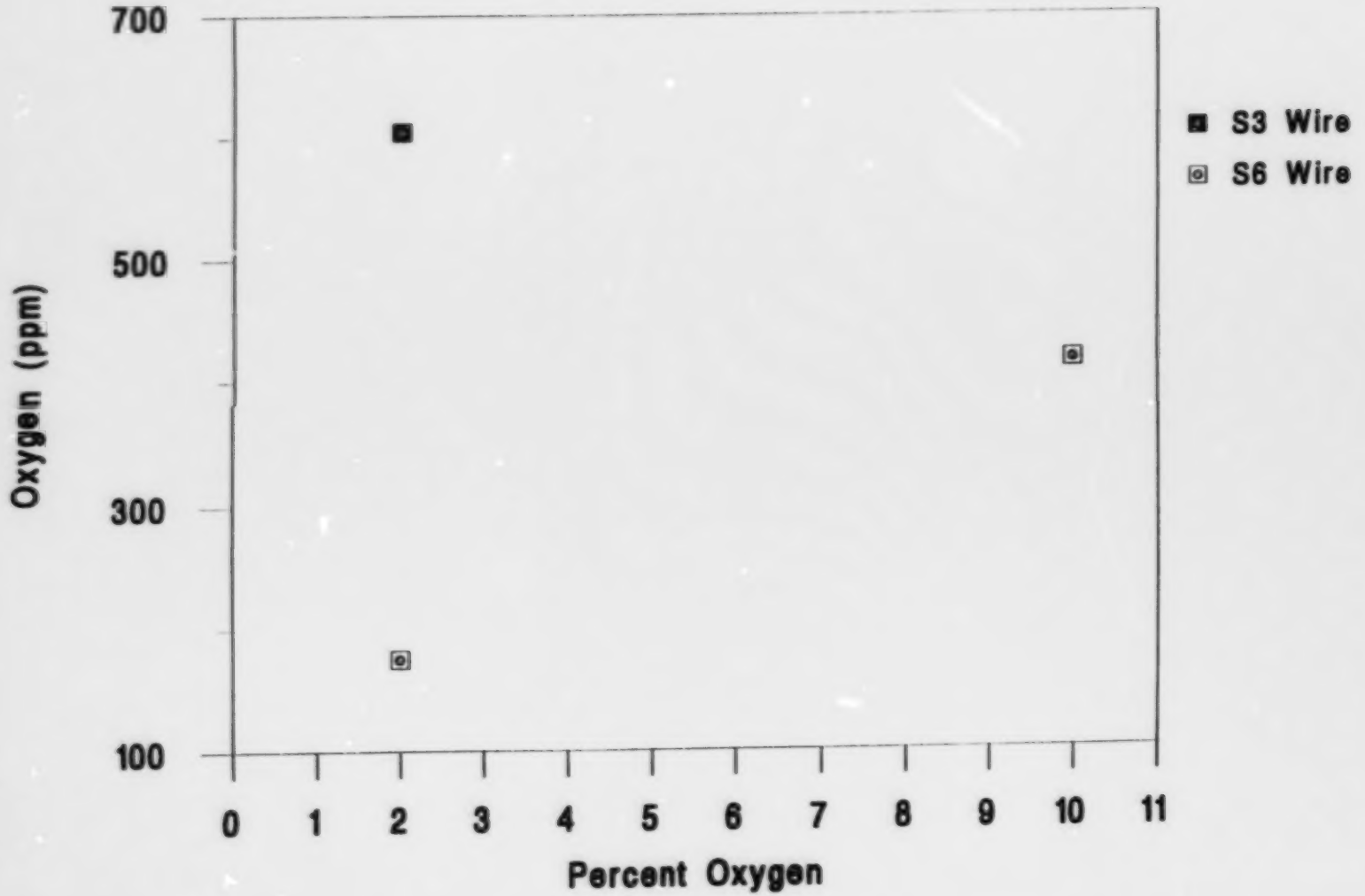

Figure 16: Weld Metal Oxygen vs. Group Index

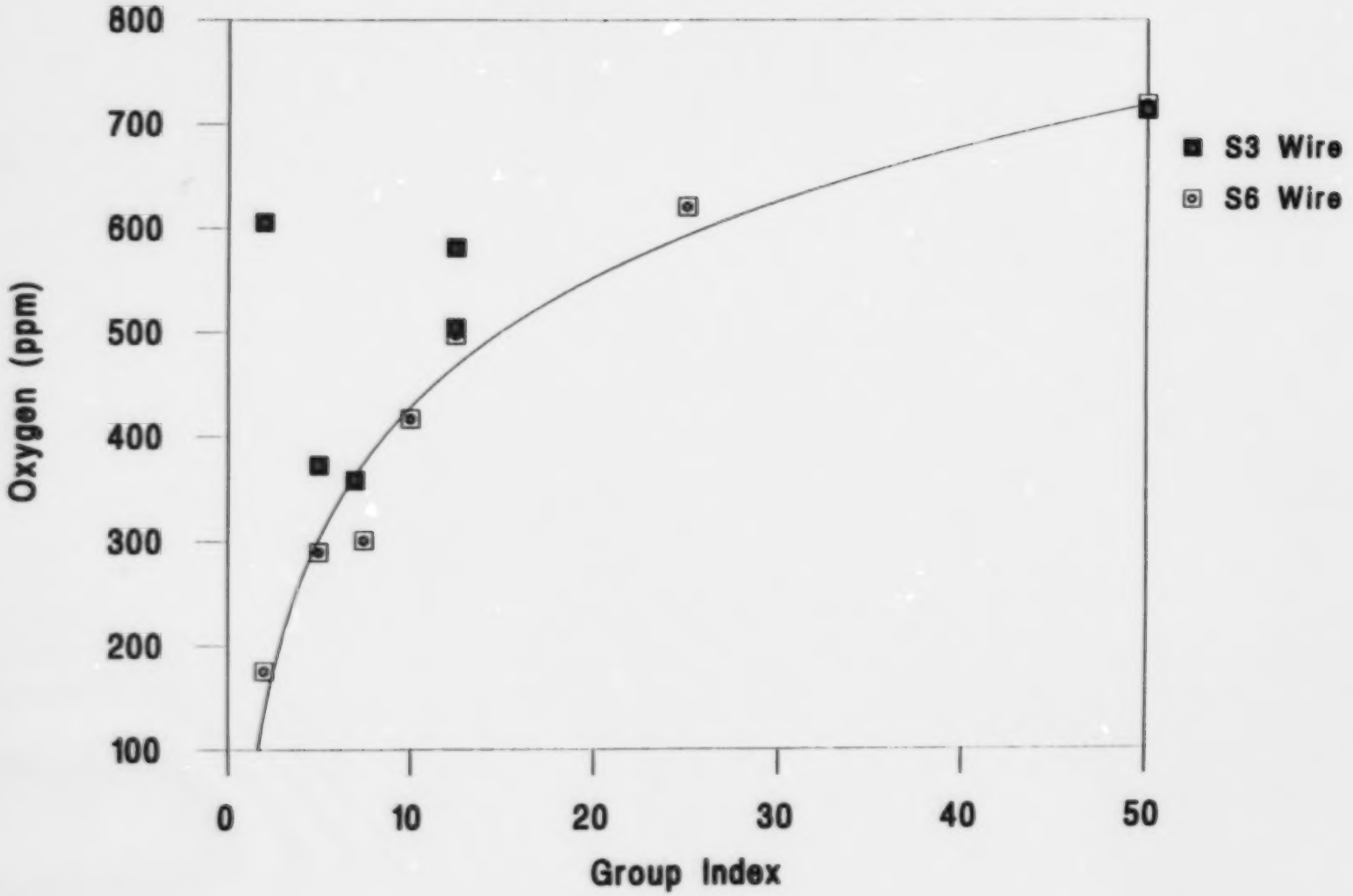

Figure 17: Weld Metal Carbon vs. Group Index

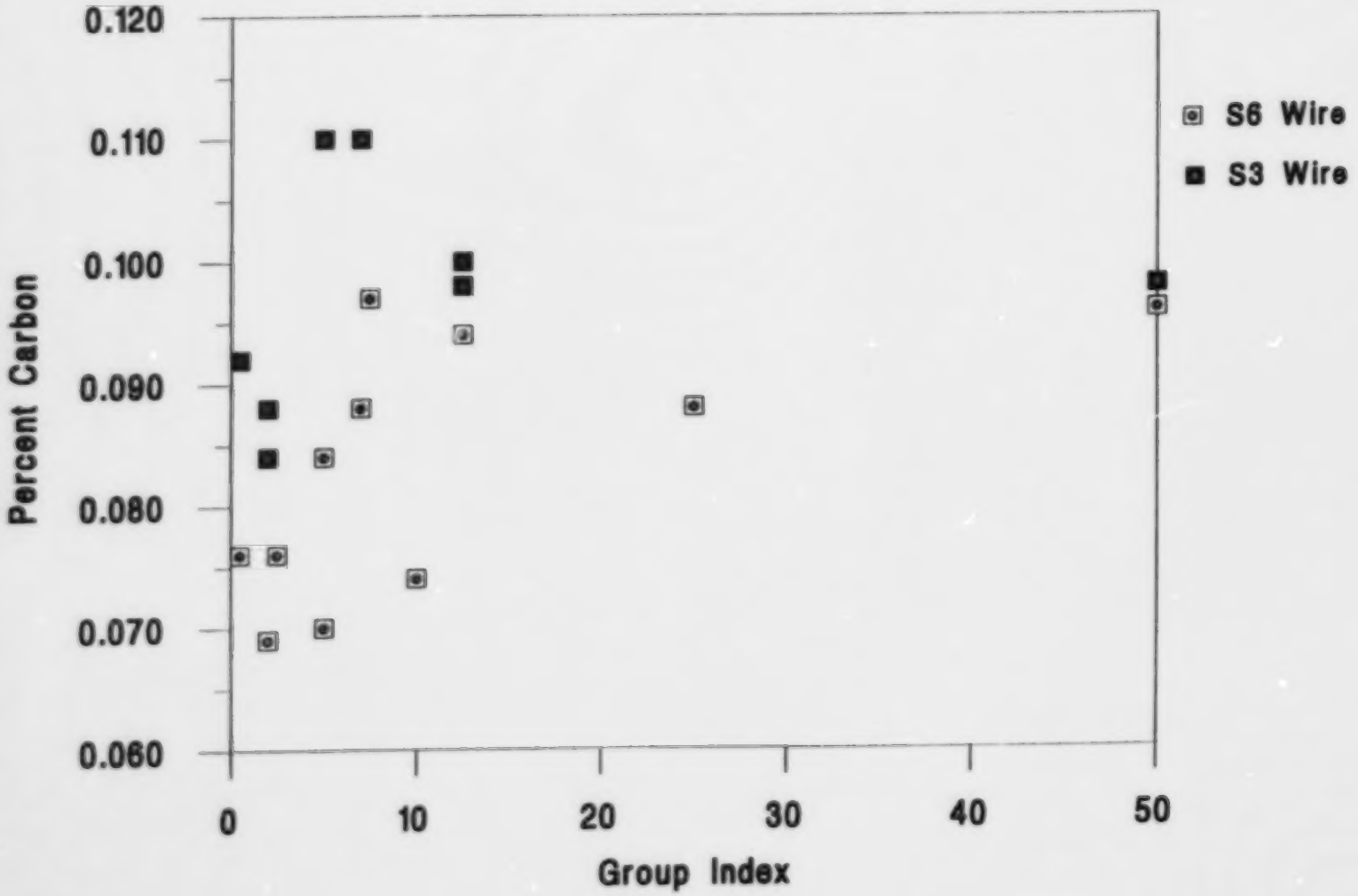

Figure 18: Weld Metal Silicon vs. Group Index

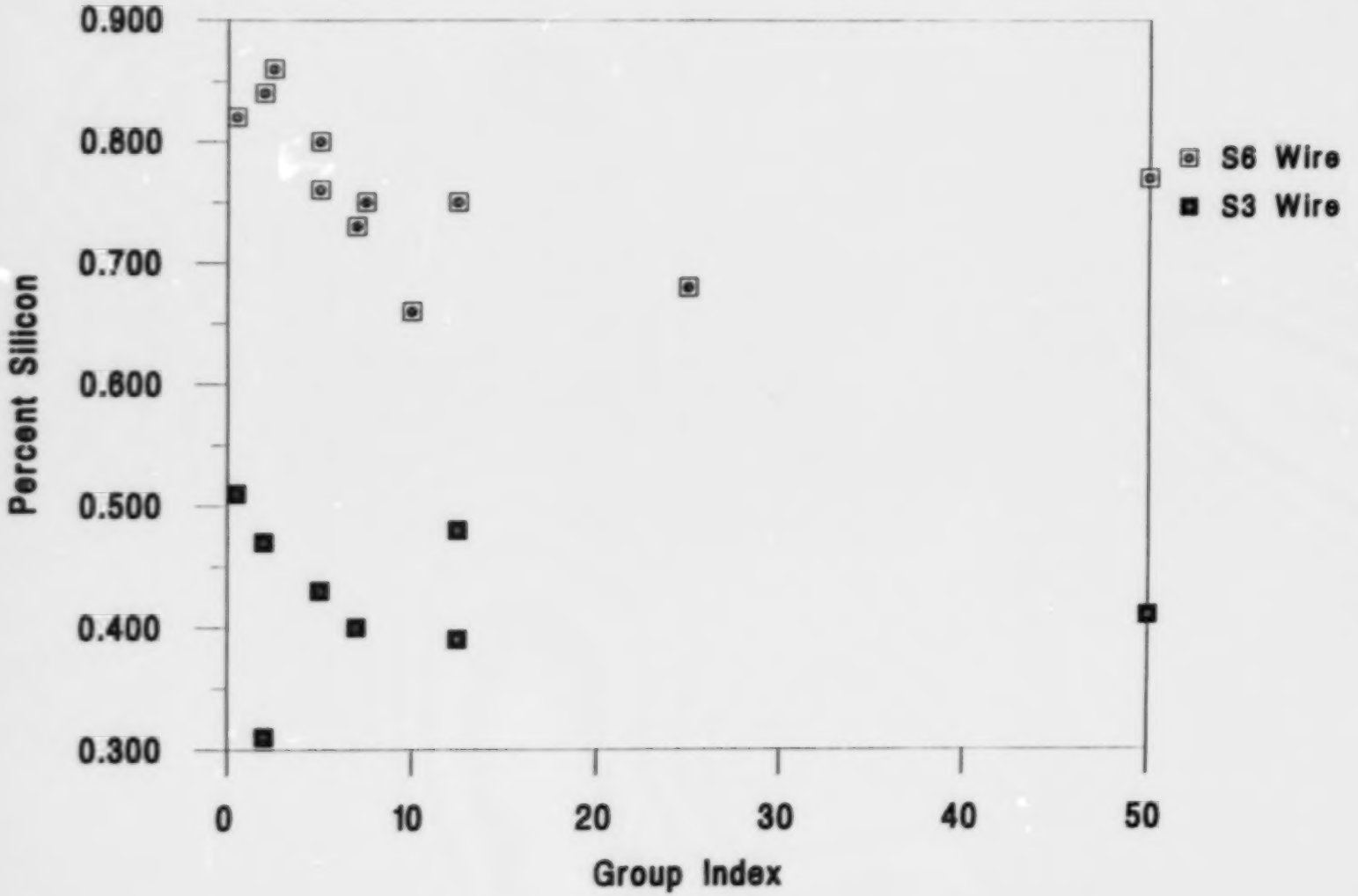

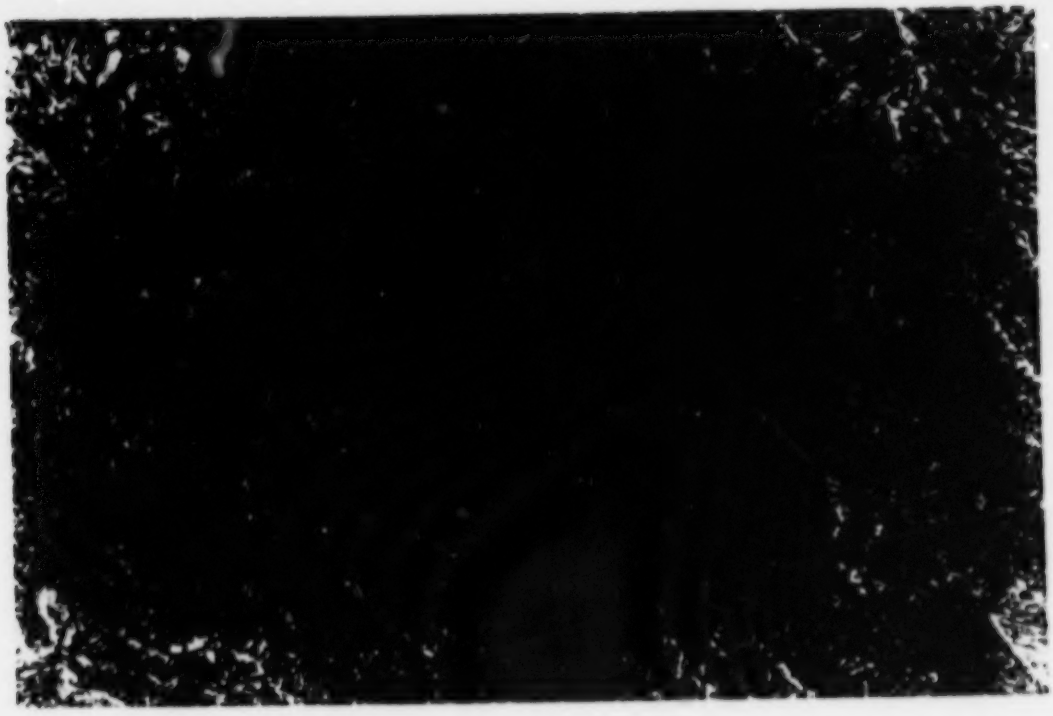

Figure 19: Micrograph of Specimen #1 (100% CO_2, S-6) 150X

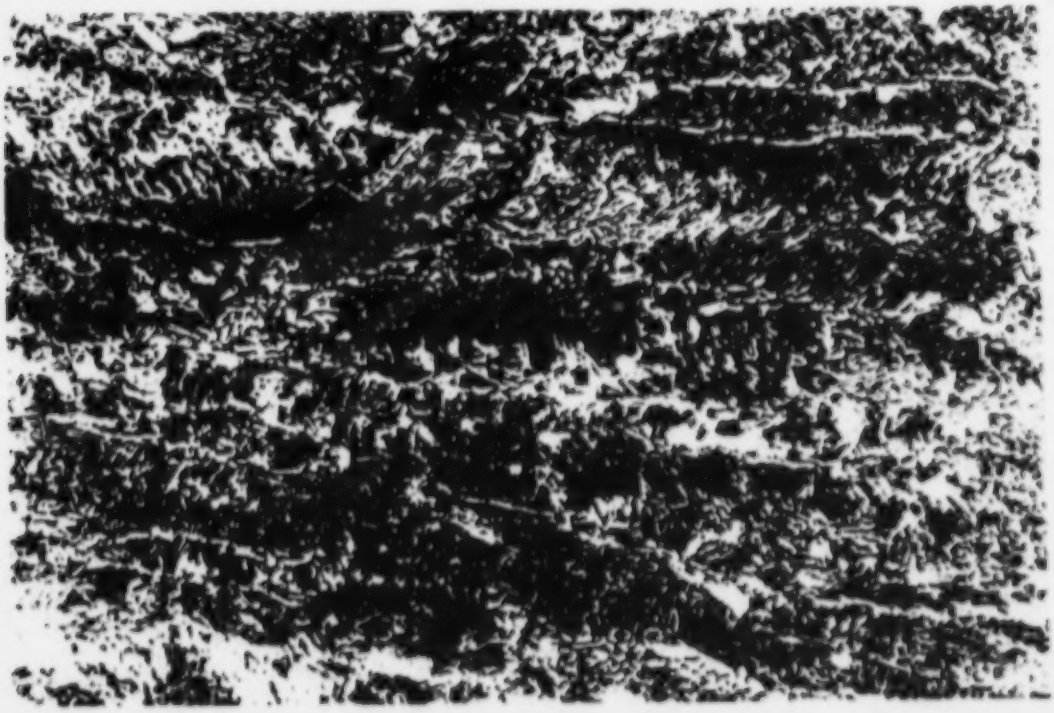

Figure 20: Micrograph of Specimen #22 (50% CO_2, Bal. Ar, S-6) 150X

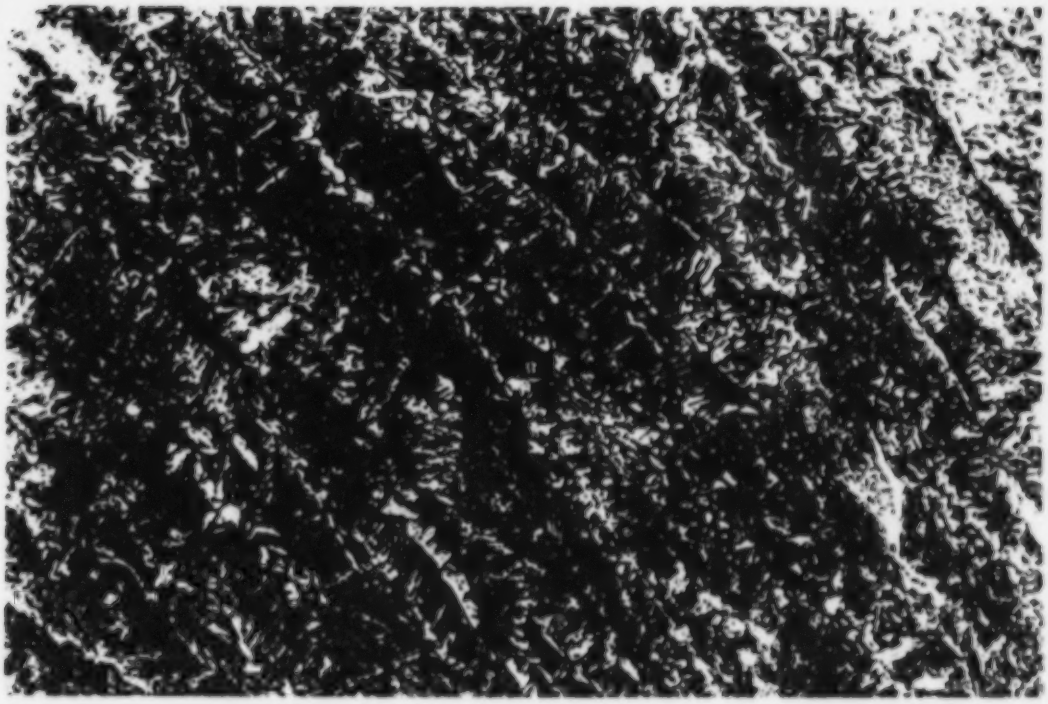

Figure 21: Micrograph of Specimen #6 (15% CO_2, Bal. Ar, S-6) 150X

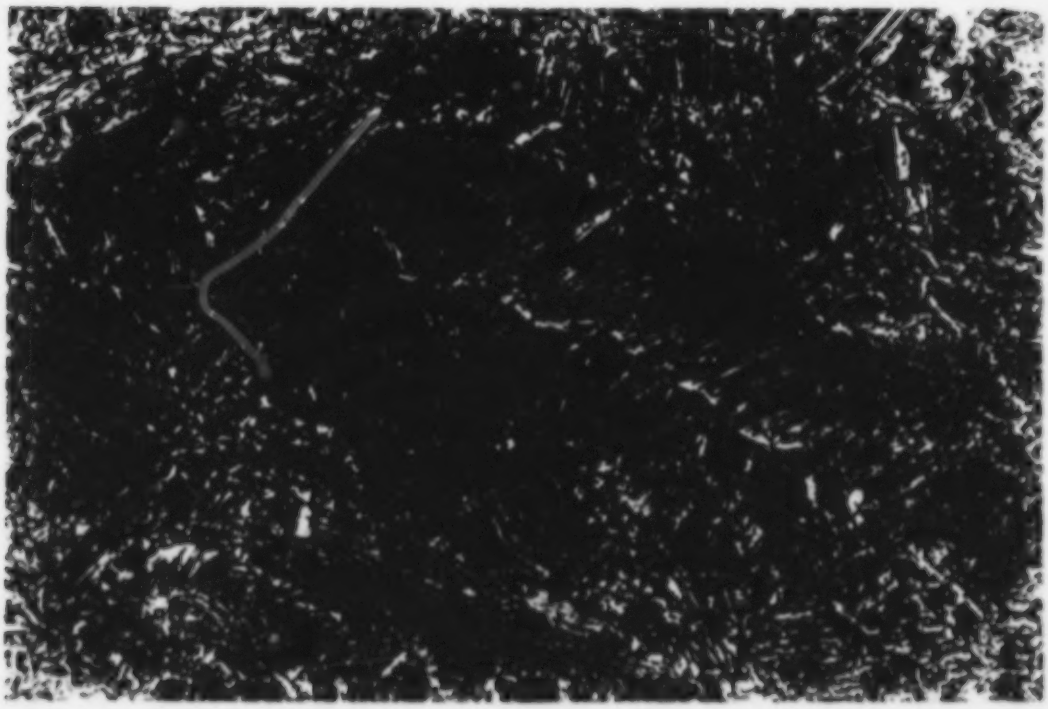

Figure 22: Micrograph of Specimen #3 (5% CO_2, Bal. Ar, S-6) 150X

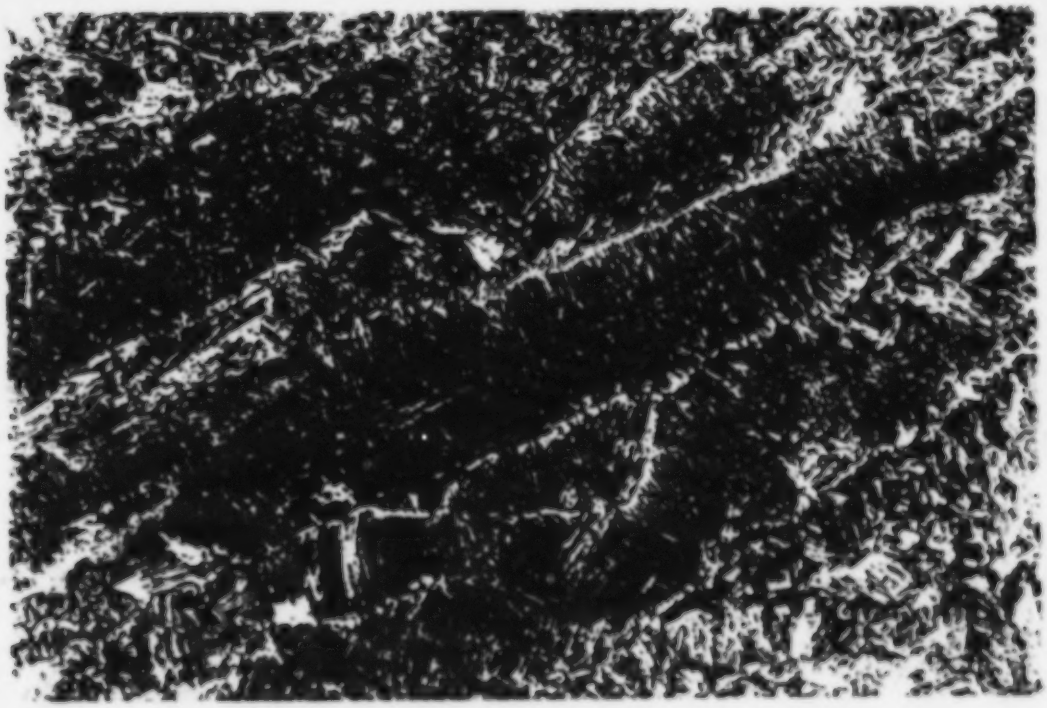

Figure 23: Micrograph of Specimen #7 (2% O_2, Bal. Ar, S-6) 150X

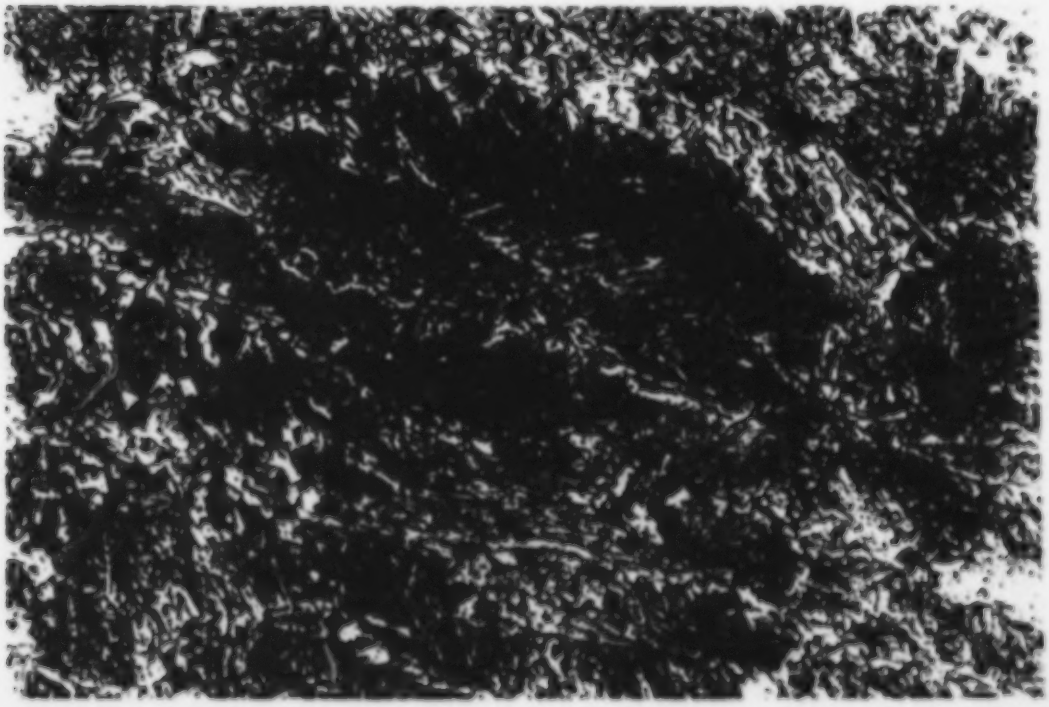

Figure 24: Micrograph of Specimen #13 (2% O_2, 10% CO_2, 30% He, Bal. Ar, S-6) 150X

Figure 25: Macrograph of Specimen #1 (100% CO_2, S-6)

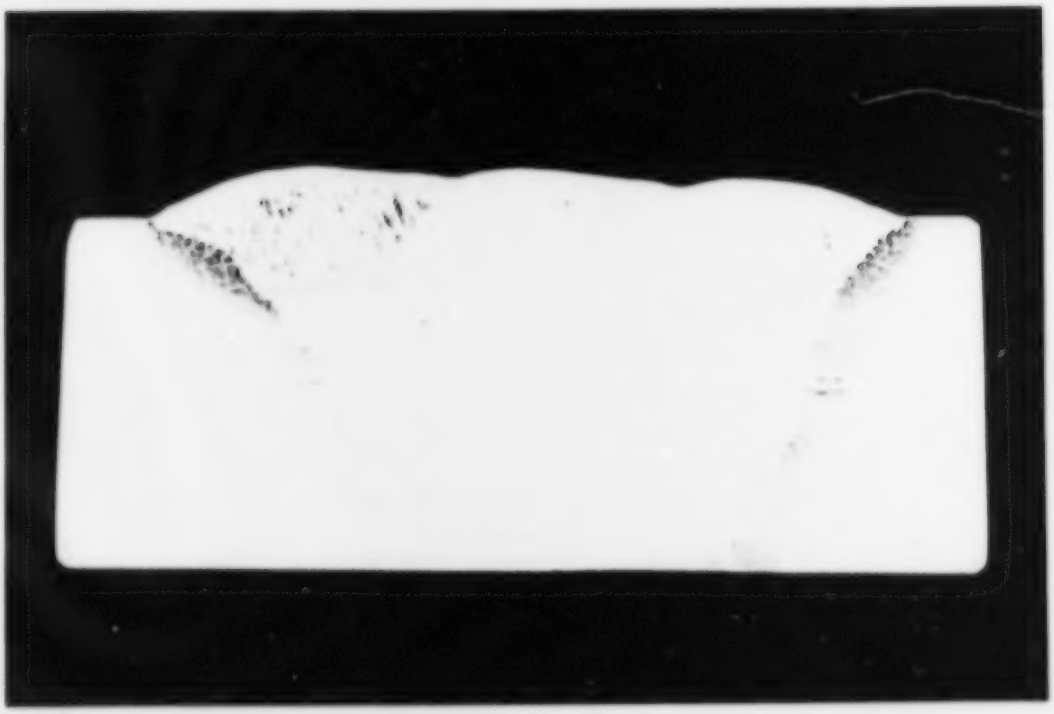

Figure 26: Macrograph of Specimen #22 (50% CO_2, Bal. Ar, S-6)

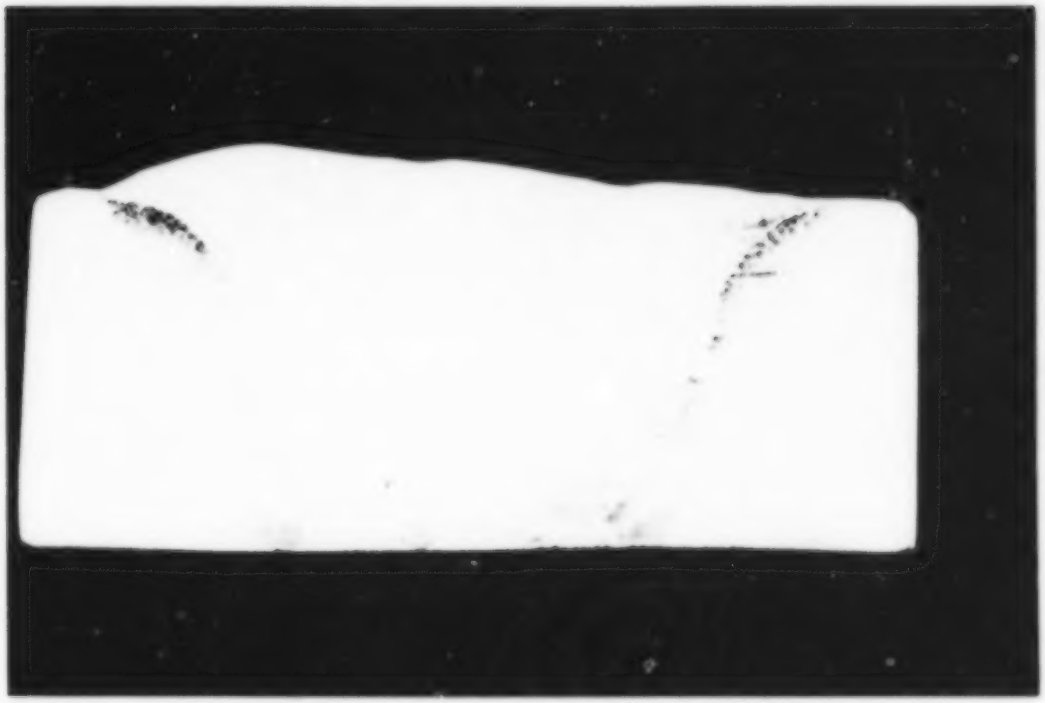

Figure 27: Macrograph of Specimen #6 (15% CO_2, Bal. Ar, S-6)

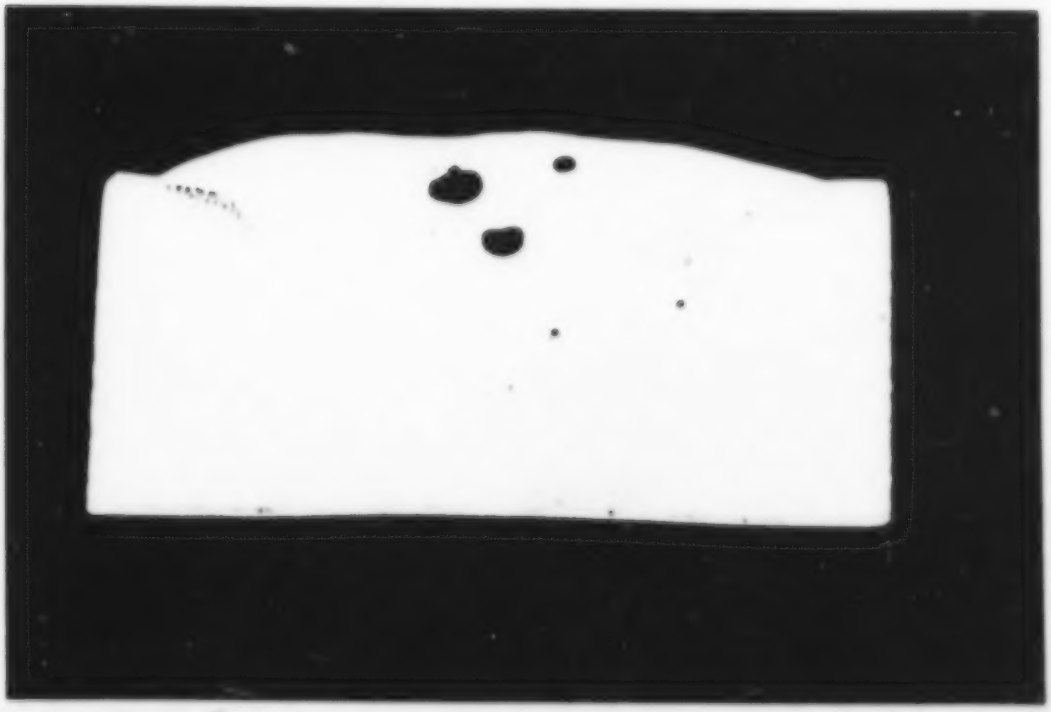

Figure 28: Macrograph of Specimen #3 (5% CO_2, Bal. Ar, S-6)

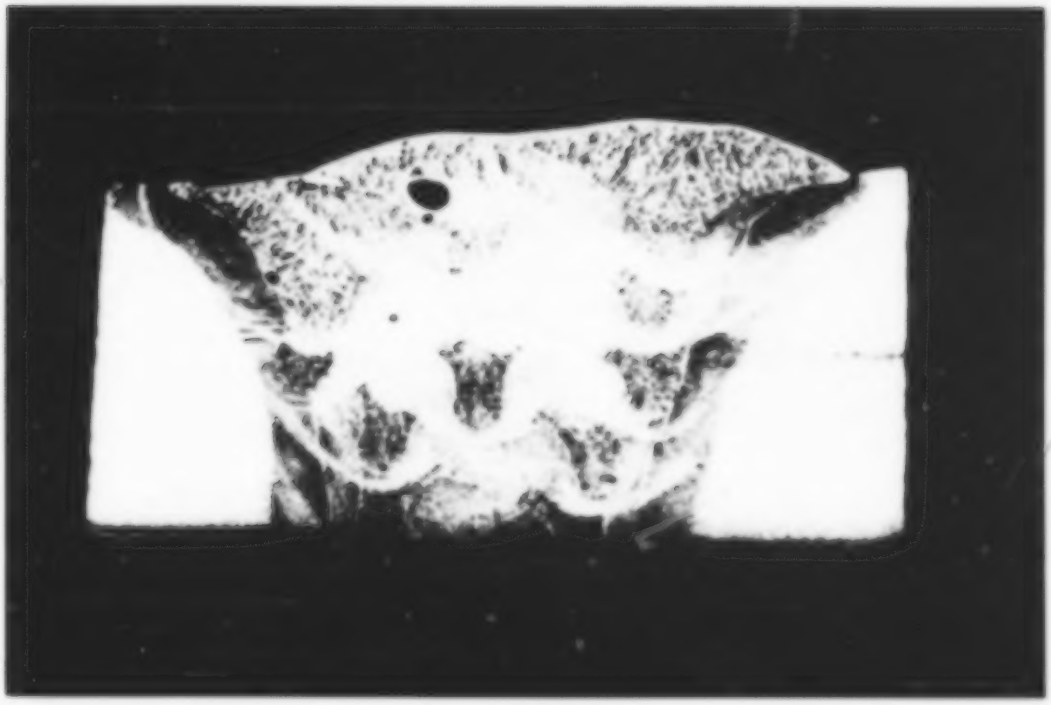

Figure 29: Macrograph of Specimen #7 ((2% O_2, Bal. Ar, S-6)

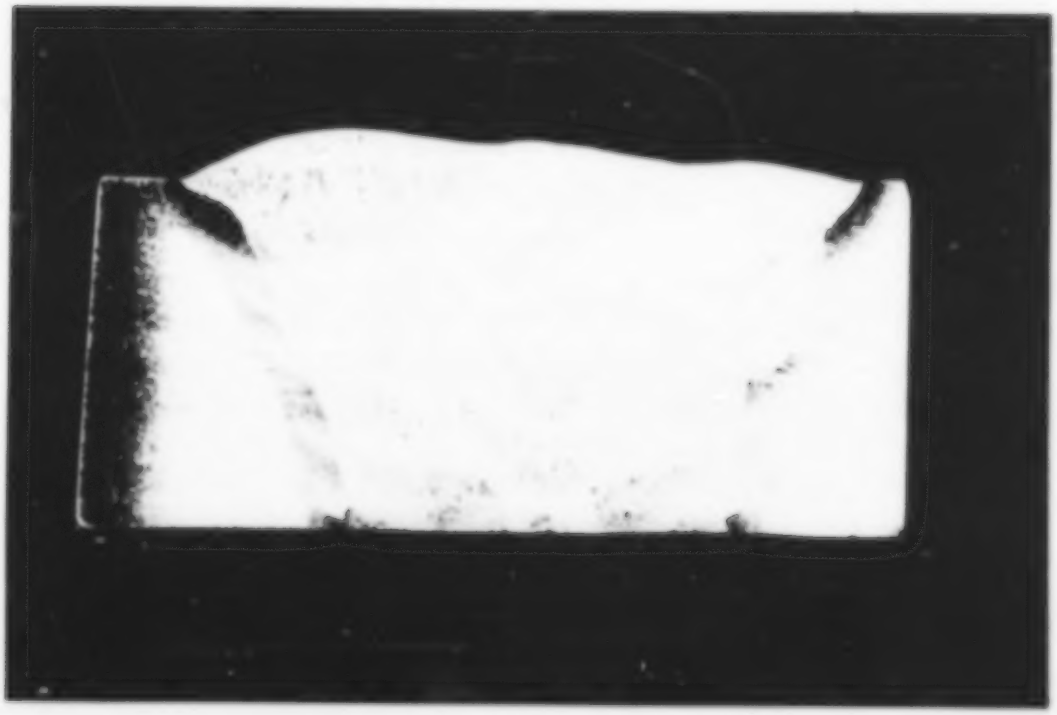

Figure 30: Macrograph of Specimen #13 (2% O_2, 10% CO_2, 30% He, Bal. Ar, S-6)

FIGURE 31

EFFECT OF SHIELDING GAS COMPOSITION ON DIFFERENCE IN HAZ